Multidimensional Orthogonal FM Transforms

Marios S. Pattichis, Alan C. Bovik, *Fellow, IEEE*, John W. Havlicek, and Nicholas D. Sidiropoulos, *Senior Member, IEEE*

***Abstract*—We present a novel class of multidimensional orthogonal FM transforms. The analysis suggests a novel signal-adaptive FM transform possessing interesting energy compaction properties. We show that the proposed signal-adaptive FM transform produces point spectra for multidimensional signals with uniformly distributed samples. This suggests that the proposed transform is suitable for energy compaction and subsequent coding of broadband signals and images that locally exhibit significant level diversity. We illustrate these concepts with simulation experiments.**

***Index Terms*—AM-FM, orthogonal transforms.**

I. Introduction

IT IS very difficult to describe nonstationary signals by expansions of stationary signals. Even wavelet expansions suffer since wavelet functions assume stationarity over the support of the function. To avoid such limitations, a multidimensional discrete amplitude and frequency-modulated (AM-FM) series expansion was first proposed in [1], where an arbitrary image is expressed as

$$I(x_1, x_2) = \sum_n a_n(x_1, x_2) \exp[j\phi_n(x_1, x_2)]. \qquad (1)$$

The amplitude functions $a_n(\cdot,\cdot)$ are assumed to be slowly-varying, and the phase functions $\phi_n(\cdot,\cdot)$ are assumed to have slowly-varying instantaneous frequency vectors $\nabla\phi_n$.

For modeling nonstationary images, AM-FM expansions of the form (1) have great potential since the amplitude and phase functions are allowed to vary continuously over the image plane. In this paper, we study a discrete version of the continuous AM-FM transform representation that was introduced in [2]. The work that we present here is a continuation of the research results in [3].

In this paper, we consider an interesting class of orthogonal FM transforms, derived from using a permutation of the signal samples followed by the DFT. In the forward transform domain, the transform is equivalent to 1) a permutation on the image samples, followed by 2) a DFT (or DCT) of the permuted samples. In the inverse transform domain, we first apply 1) a DFT (or DCT), followed by 2) the inverse permutation (the inverse of the permutation in Step 1) of the forward transform).

One-dimensional AM-FM expansions have also been studied in [4], [5] and [6], where one-dimensional AM-FM expansions were expressed in terms of frequency-amplitude modulated (FAM) complex exponentials. The class of FAM functions is indexed by a parameter α, and the FAM functions are expressed as: $\mathrm{FAM}(\alpha, x) = \sqrt{dg(x)/dx}\exp[j\alpha g(x)]$. When the FAM set is designed in the frequency domain, the set of functions is called FAMlets. FAM functions have also found applications in signal compression. The FAM functions have the limitation, however, that the AM and FM terms are coupled.

More general classes of one-dimensional (1-D) AM-FM expansions are also presented in [7]. The authors suggest that a large class of signal processing algorithms can be thought of as being composed of three general steps: 1) applying a unitary transformation to the signal or image, 2) processing the transformed signal or image, and possibly 3) transforming the result back. In this general scheme, our method considers permutations as the unitary transformation. The authors of [7] have also presented a variety of important time-warping functions that are associated with 1-D FM signals that have been studied in the literature.

The multidimensional FM expansions that we present here are fundamentally different from those in other studies: since permutations have no continuous-space analogue, our expansions have no continuous counterpart. Hence, this class of FM transforms provides a novel approach to the problem of expanding signals as a sum of multidimensional FM series. The analysis suggests a novel signal-adaptive FM transform possessing interesting energy compaction properties. We show that the proposed signal-adaptive FM transform produces point spectra for multidimensional signals with uniformly distributed samples, and very narrowband spectra for signals with approximately uniformly distributed samples. These results suggest that the proposed transform is suitable for energy compaction and subsequent coding of broadband, noise-like signals and images. We illustrate these concepts with simulation experiments.

We organize the rest of the paper in four sections. In Section II, we derive the general conditions for designing multidimensional, orthogonal FM transforms. We also consider some classes of FM transforms that are of special interest. We present examples of two dimensional FM transforms in Section V. In Section VI, we describe an example where a two dimensional FM transform is implemented, and then compare the performance to JPEG. In Section VII, we summarize our description

Manuscript received September 23, 1999; revised September 22, 2000. This work was supported in part by the Air Force Office of Scientific Research, Air Force Systems Command, USAF, under Grant Number F49620-93-1-0307, and by the Army Research Office under Contract DAAH 049510494. The associate editor coordinating the review of this manuscript and approving it for publication was Prof. Glenn Healey.

M. S. Pattichis is with the Department of Electrical and Computer Engineering, University of New Mexico, Albuquerque, NM 87131-1356 USA (e-mail: pattichis@eece.unm.edu).

A. C. Bovik is with the Department of Electrical and Computer Engineering, University of Texas at Austin, Austin, TX 78712 USA (e-mail: bovik@ece.utexas.edu).

J. W. Havlicek is with Motorola, Inc., Austin, TX 78729 USA (e-mail: havlicek@adtx.sps.mot.com).

N. D. Sidiropoulos is with the Department of Electrical Engineering, University of Virginia, Charlottesville, VA 22903 (e-mail: nikos@virginia.edu).

Publisher Item Identifier S 1057-7149(01)00821-1.

for the FM transform coding example, and briefly comment on future research on FM transforms.

II. FM Transforms

Let $x(\cdot)$ be a bounded M-dimensional signal with domain the discrete hypercube $Q = \{0, 1, \ldots, N-1\}^M$. This means that $x(\cdot)$ is a function such that, for every $q \in Q$, $x(\cdot)$ is a complex number. Later, we will understand that $Q = (\mathcal{Z}/N)^M$, where $\mathcal{Z}/N$ denotes the ring of integers modulo N. Motivated by coding applications, we are interested in expressing $x(\cdot)$ as a sum of FM components

$$x(\mathbf{n}) = \frac{1}{K_{\mathbf{\Phi}}} \sum_{\mathbf{k} \in Q} X(\mathbf{k}) \exp\left[j \frac{2\pi}{N} \mathbf{k} \cdot \mathbf{\Phi}(\mathbf{n}) \right] \tag{2}$$

such that the FM spectrum $X(\cdot)$ can be computed using

$$X(\mathbf{k}) = \frac{1}{K_{\mathbf{\Phi}}} \sum_{\mathbf{n} \in Q} x(\mathbf{n}) \exp\left[-j \frac{2\pi}{N} \mathbf{k} \cdot \mathbf{\Phi}(\mathbf{n}) \right]. \tag{3}$$

Here, $\mathbf{n} = (n_1, n_2, \ldots, n_M)$ and $\mathbf{k} = (k_1, k_2, \ldots, k_M)$ denote elements of Q. We understand that the FM phase function $\mathbf{\Phi}(\cdot) = (\phi_1(\cdot), \phi_2(\cdot), \ldots, \phi_M(\cdot))$ takes values in $(\mathcal{R}/N)^M$, where $\mathcal{R}$ is the real line. Also, we use "$\cdot$" to denote the standard inner product reduced $\bmod N$

$$\mathbf{k} \cdot \mathbf{\Phi}(\mathbf{n}) = k_1\phi_1(\mathbf{n}) + k_2\phi_2(\mathbf{n}) + \cdots + k_M\phi_M(\mathbf{n}) \bmod N.$$

In (2), the $\mathbf{k}$th FM component $\exp[-j(2\pi/N)\mathbf{k} \cdot \mathbf{\Phi}(\cdot)]$ is weighted by the corresponding FM spectral coefficient $X(\mathbf{k})$, and the sum of these contributions over all $\mathbf{k} \in Q$ synthesizes the original signal $x(\cdot)$. The FM spectrum $X(\cdot)$ depends on the choice of $\mathbf{\Phi}(\cdot)$. Thus, the FM transform is actually a *class* of transforms; a particular instance is specified by selecting an $(\mathcal{R}/N)^M$-valued phase function $\mathbf{\Phi}(\cdot)$ and kernel constant $K_{\mathbf{\Phi}} > 0$ such that the synthesis formula (2) and the analysis formula (3) hold for an arbitrary bounded signal $x(\cdot)$. The dependence of $X(\cdot)$ on $\mathbf{\Phi}(\cdot)$ should be understood and is not generally written explicitly.

The following proposition clarifies the dependence of the FM transform on the choices of $\mathbf{\Phi}(\cdot)$ and $K_{\mathbf{\Phi}}$.

Proposition 1 (Uniqueness): Let $\mathbf{\Phi}, \mathbf{\Psi} : Q \to (\mathcal{R}/N)^M$, and let $\mathcal{F}_{\mathbf{\Phi}}, \mathcal{F}_{\mathbf{\Psi}}$ denote associated FM transforms. Then $\mathcal{F}_{\mathbf{\Phi}} = \mathcal{F}_{\mathbf{\Psi}}$ if and only if $K_{\mathbf{\Phi}} = K_{\mathbf{\Psi}}$ and $\mathbf{\Phi} = \mathbf{\Psi} \bmod N$.

Proof: Suppose $\mathcal{F}_{\mathbf{\Phi}} = \mathcal{F}_{\mathbf{\Psi}}$. Applying both transforms to $\delta(\mathbf{n} - \mathbf{p})$ gives

$$\frac{1}{K_{\mathbf{\Phi}}} \exp\left[-j \frac{2\pi}{N} \mathbf{k} \cdot \mathbf{\Phi}(\mathbf{p}) \right] = \frac{1}{K_{\mathbf{\Psi}}} \exp\left[-j \frac{2\pi}{N} \mathbf{k} \cdot \mathbf{\Psi}(\mathbf{p}) \right]$$

for all $\mathbf{k}, \mathbf{p} \in Q$. Putting $\mathbf{k} = \mathbf{0}$, we conclude that $K_{\mathbf{\Phi}} = K_{\mathbf{\Psi}}$, and so

$$\exp\left[-\frac{2\pi}{N} j \mathbf{k} \cdot \mathbf{\Phi}(\mathbf{p}) \right] = \exp\left[-\frac{2\pi}{N} j \mathbf{k} \cdot \mathbf{\Psi}(\mathbf{p}) \right]$$

for all $\mathbf{k}, \mathbf{p} \in Q$. Now put $\mathbf{k} = \mathbf{e}_a$, the ath standard unit vector, to get

$$\exp\left[-\frac{2\pi}{N} j \phi_a(\mathbf{p}) \right] = \exp\left[-\frac{2\pi}{N} j \psi_a(\mathbf{p}) \right]$$

for all $a \in \{1, \ldots, M\}$ and all $\mathbf{p} \in Q$. This implies that $\mathbf{\Phi} = \mathbf{\Psi} \bmod N$.

The converse is obvious. Q.E.D.

Next, we derive a general orthonormality condition.

Proposition 2 (Orthonormality Condition): Assume that $\mathbf{\Phi}$ satisfies

$$\frac{1}{K_{\mathbf{\Phi}}^2} \sum_{\mathbf{k} \in Q} \exp\left[j \frac{2\pi}{N} \mathbf{k} \cdot (\mathbf{\Phi}(\mathbf{n}) - \mathbf{\Phi}(\mathbf{p})) \right] = \delta(\mathbf{n} - \mathbf{p}) \tag{4}$$

for all $\mathbf{n}, \mathbf{p} \in Q$, where $\delta(\cdot)$ denotes the Kronecker delta function. Then any bounded signal $x(\cdot)$ on Q is given by

$$x(\mathbf{n}) = \frac{1}{K_{\mathbf{\Phi}}} \sum_{\mathbf{k} \in Q} X(\mathbf{k}) \exp\left[j \frac{2\pi}{N} \mathbf{k} \cdot \mathbf{\Phi}(\mathbf{n}) \right] \tag{5}$$

where the FM spectrum is given by

$$X(\mathbf{k}) = \frac{1}{K_{\mathbf{\Phi}}} \sum_{\mathbf{n} \in Q} x(\mathbf{n}) \exp\left[-j \frac{2\pi}{N} \mathbf{k} \cdot \mathbf{\Phi}(\mathbf{n}) \right]. \tag{6}$$

Proof: The proof follows after using (6) to substitute for $X(\mathbf{k})$, in the right-hand side of (5).

For 1-D FM transforms, the form of $\mathbf{\Phi}$ is determined by the following proposition. □

Proposition 3 (Orthonormal FM Transforms in One Dimension): Let $M = 1$. Then the orthonormal condition (4) is satisfied if and only if $\mathbf{\Phi}(i) = \sigma(i) + \beta \bmod N$ for some permutation σ of $\{0, 1, \ldots, N-1\}$ and some real number β. Furthermore, the kernel constant is given by $K_{\mathbf{\Phi}} = \sqrt{N}$.

Proof: The proof is straightforward and has been omitted. □

Proposition 4: If $\phi(\cdot)$ is a permutation of $\{0, \ldots, N-1\}$, then the associated one-dimensional FM transform is equivalent to a permutation of signal samples followed by the ordinary DFT.

Proof: The proof is straightforward and has been omitted. □

We now generalize Proposition 3 to multiple dimensions.

Theorem 1 (Multidimensional Orthonormal FM Transforms): Let $K_{\mathbf{\Phi}} = N^{M/2}$, where M is the number of spatial dimensions. Let $\mathbf{\Phi} = (\phi_1, \ldots, \phi_M)$. Then $\mathbf{\Phi}$ satisfies the orthonormal condition (4) if and only if there is a symmetric function $\alpha : Q \times Q \to \{1, \ldots, M\}$ such that

$$\phi_{\alpha(\mathbf{n},\mathbf{p})}(\mathbf{n}) - \phi_{\alpha(\mathbf{n},\mathbf{p})}(\mathbf{p})$$

is a nonzero integer $\bmod N$ whenever $\mathbf{n} \neq \mathbf{p}$. [By *symmetric*, we mean that $\alpha(\mathbf{n}, \mathbf{p}) = \alpha(\mathbf{p}, \mathbf{n})$ for all $\mathbf{n}, \mathbf{p} \in Q$.]

Proof: Since $K_{\mathbf{\Phi}} = N^{M/2}$, (4) is satisfied whenever $\mathbf{n} = \mathbf{p}$. For $\mathbf{n} \neq \mathbf{p}$, (4) is satisfied if and only if

$$\begin{aligned}
0 &= \sum_{\mathbf{k}\in Q} \exp\left[j\frac{2\pi}{N}\mathbf{k}\cdot(\mathbf{\Phi}(\mathbf{n}) - \mathbf{\Phi}(\mathbf{p}))\right] \\
&= \sum_{\mathbf{k}\in Q}\prod_{a=1}^{M} \exp\left[j\frac{2\pi}{N}k_a(\phi_a(\mathbf{n}) - \phi_a(\mathbf{p}))\right] \\
&= \sum_{k_1=0}^{N-1}\cdots\sum_{k_M=0}^{N-1}\prod_{a=1}^{M} \exp\left[j\frac{2\pi}{N}k_a(\phi_a(\mathbf{n}) - \phi_a(\mathbf{p}))\right] \\
&= \left(\sum_{k_1=0}^{N-1} \exp\left[j\frac{2\pi}{N}k_1(\phi_1(\mathbf{n}) - \phi_1(\mathbf{p}))\right]\right) \\
&\quad \cdots \left(\sum_{k_M=0}^{N-1} \exp\left[j\frac{2\pi}{N}k_M(\phi_M(\mathbf{n}) - \phi_M(\mathbf{p}))\right]\right) \\
&= \prod_{a=1}^{M}\left(\sum_{k=0}^{N-1} \exp\left[j\frac{2\pi}{N}k(\phi_a(\mathbf{n}) - \phi_a(\mathbf{p}))\right]\right).
\end{aligned}$$

This last expression is zero if and only if a factor

$$\sum_{k=0}^{N-1} \exp\left[j\frac{2\pi}{N}k(\phi_a(\mathbf{n}) - \phi_a(\mathbf{p}))\right] = 0 \tag{7}$$

for some index $a \in \{1,\ldots,M\}$, which may depend on $(\mathbf{n},\mathbf{p})$. But, as we have seen, (7) holds if and only if $\phi_a(\mathbf{n}) - \phi_a(\mathbf{p})$ is a nonzero integer $\bmod N$. The relation $(\mathbf{n},\mathbf{p}) \mapsto a$ defines the function α for $\mathbf{n} \neq \mathbf{p}$; $\alpha(\mathbf{n},\mathbf{n})$ can be defined arbitrarily. Since $\phi_a(\mathbf{n}) - \phi_a(\mathbf{p})$ is a nonzero integer $\bmod N$ if and only if $\phi_a(\mathbf{p}) - \phi_a(\mathbf{n})$ is a nonzero integer $\bmod N$, the existence of α is equivalent to the existence of a symmetric α. Q.E.D.

Remark 1: Note that the existence of α implies that $\mathbf{\Phi}$ is one-to-one.

As in the 1-D case, choosing $\mathbf{\Phi}(\cdot)$ to be a permutation of Q ensures that the orthonormal condition is satisfied.

Proposition 5: If $\mathbf{\Phi}(\cdot)$ is a permutation of Q, then the M-dimensional FM transform is equivalent to a permutation of signal samples followed by the M-dimensional DFT.

Proof: Similar to the proof for the one-dimensional case. Q.E.D.

III. FM Transforms from Permutations

For the remainder of this paper, we focus on FM transforms built from phase functions $\mathbf{\Phi}$ that are permutations of Q. We also identify Q with $(\mathcal{Z}/N)^M$. According to Proposition 5, such a transform is equivalent to permuting the input signal and then applying the ordinary DFT. Thus, it is of interest to identify signals whose DFT spectra are sparse to serve as *targets* for signal permutation. Once a collection of target signals is chosen, a general signal-adaptive transform strategy is to *match* an input signal via permutation to a target signal that is "close" and then apply the DFT. This strategy was introduced in [3] for one-dimensional signals.

We begin by identifying a family of signals on Q whose DFT spectra are sparse. It will be convenient to write $Q' = (\mathcal{Z}/N)^{M-1}$ and $\mathbf{n}' = (n_2,\ldots,n_M)$.

Definition 1 (Unidirectional Periodic Signal): A *unidirectional periodic signal* $x(\cdot)$ is any signal on Q that satisfies

1) $x(\mathbf{n})$ depends only on the first coordinate n_1 of $\mathbf{n}$, i.e., $x(\mathbf{n}) = x(\mathbf{p})$ if $n_1 = p_1$. We will abuse notation in this case and write $x(\mathbf{n}) = x(n_1)$.
2) For some positive integer T dividing N, $x(\cdot)$ is T-periodic in its first coordinate: $x(n_1) = x(n_1 + T)$.

If, in addition to 1 and 2, $x(0), x(1), \ldots, x(T-1)$ are distinct, then $x(\cdot)$ is said to be a *proper* unidirectional periodic signal.

To emphasize the period, we may say that a signal is unidirectional T-periodic. In two-dimensions, if n_1 denotes the column coordinate, we note that target signals remain invariant throughout a column. Hence, as we shall see, for the least-squares optimal permutation, we will permute image samples with similar intensity to the same column, allowing sequential memory accesses to the target signal.

Proposition 6 (Spectrum of Unidirectional Periodic Signals): Let $x(\cdot)$ be a unidirectional T-periodic signal on Q. Then, the DFT $X(\cdot)$ of $x(\cdot)$ satisfies $X(\mathbf{k}) = 0$ if either N/T does not divide k_1 or $\mathbf{k}' \neq \mathbf{0}$ (i.e., at least one of $k_2,\ldots,k_M$ is nonzero).

Proof: Since $x(\cdot)$ depends only on the first coordinate, it is clear that $X(\mathbf{k}) = 0$ if $\mathbf{k}' \neq \mathbf{0}$. Now, assume N/T does not divide k_1. Then

$$\begin{aligned}
X(\mathbf{k}) &= \frac{1}{K_{\mathbf{\Phi}}} \sum_{\substack{0\le\nu\le T-1\\ 0\le\mu\le(N/T)-1}} \sum_{\mathbf{n}'\in Q'} x(\mu T+\nu,\mathbf{n}') \\
&\quad \times \exp\left[j\frac{2\pi}{N}(k_1(\mu T+\nu) + \mathbf{k}'\cdot\mathbf{n}')\right] \\
&= \frac{1}{K_{\mathbf{\Phi}}} \sum_{\mathbf{n}'\in Q'}\sum_{\nu=0}^{T-1} x(\nu,\mathbf{n}') \exp\left[j\frac{2\pi}{N}(k_1\nu + \mathbf{k}'\cdot\mathbf{n}')\right] \\
&\quad \times \sum_{\mu=0}^{N/T-1} \exp\left[j\frac{2\pi}{N}k_1\mu T\right].
\end{aligned}$$

Consider the terms in the last sum. Since N/T does not divide k_1, the integers

$$0, k_1T, 2k_1T, \ldots, ((N/T)-1)k_1T$$

are all distinct $\bmod N$. Applying $\exp[j(2\pi/N)(\cdot)]$ yields

$$1, W_N^{k_1T}, W_N^{2k_1T}, \ldots, W_N^{(N/T-1)k_1T},$$

where we have written W_N for $\exp[j(2\pi/N)(\cdot)]$. These numbers are the complex (N/T)th roots of unity, whose sum is zero. Q.E.D.

Proposition 7 (Uniformly Distributed Signals): Let T divide N. A signal $x(\cdot)$ on Q can be permuted to a unidirectional (respectively, proper unidirectional) T-periodic signal if and only if $x(\cdot)$ assumes at most (respectively, exactly) T distinct values, each with multiplicity a positive multiple of N^M/T.

Proof: Let $x(\cdot)$ be a proper unidirectional periodic signal. Let $x(\mathbf{n}_0)$ be a particular sample of $x(\cdot)$. that $x(\cdot)$ assumes T distinct values with multiplicity N^m/T. Let x_i be one of the T values. We can place x_i at $x(i, n_2, \ldots, n_M), \ldots, x(i+(N/T-1)T,), 0 \le n_2,\ldots,n_M \le N-1$. Similarly, we can place all T

distict values, and the resulting signal will be proper unidirectional periodic.

Next we consider the case when $x(\cdot)$ assumes at-most T distinct values. Let x_i be a value repeating mN^M/T times where m is a positive integer. Then, we think of x_i as m copies of a value that repeats N^M/T times, and proceed in the same way as we have just described for the proper case. Q.E.D.

Propositions 7 and 6 imply that signals with $T \mid N$ uniformly distributed samples can be represented using very few coefficients *in a suitable FM transform domain*, namely, using the FM transform associated to the permutation that makes the signal unidirectional. This permutation and its inverse are easy to find, as shown in [3]. This observation suggests the use of a *signal-adaptive* FM transform, in which $\mathbf{\Phi}(\cdot)$ is a function of the input. In practice, of course, the matching of signals by permutation will only be approximate, and the specification of $\mathbf{\Phi}(\cdot)$ may actually carry a significant part of the representation (coding) cost. Nevertheless, as demonstrated in [3], and to a greater extent herein, there are important rate-distortion gains to be derived from this approach.

Next, we will prove an invariance property for signal-adaptive FM spectra. Low variation in the spectra of a sequence of signals is desirable since techniques such as DPCM can be used to reduce the cost of coding the sequence, thereby offsetting in part the overhead of representing permutations. First, we need some definitions. Let x, t be signals on Q (we think of t as the "target" signal). If the permutation $\mathbf{\Phi}$ of Q minimizes the energy quantity

$$\sum_{\mathbf{k}\in Q}(x(\mathbf{\Phi}(\mathbf{k}))-t(\mathbf{k}))^2 \tag{8}$$

then we say that $\mathbf{\Phi}$ *matches* x to t. In case the identity permutation matches x to t, then we say x and t are *matched*. Matching permutations can always be found by using sorting [3]. To make this precise, we fix a bijection

$$\beta: Q \to \{1,\ldots,N^M\}.$$

Q is then ordered by defining $\mathbf{k} \le \mathbf{n}$ iff $\beta(\mathbf{k}) \le \beta(\mathbf{n})$. The bijection serves as an index for multidimensional arrays. As an example, for accessing multidimensional arrays declared in a computer language like "C", the bijection is defined from the M-dimensional array index to an offset from the base address of the array.

A signal x on Q is *sorted* provided

$$\mathbf{k} \le \mathbf{n} \Rightarrow x(\mathbf{k}) \le x(\mathbf{n})$$

and a permutation $\mathbf{\Phi}$ *sorts* x provided $x(\mathbf{\Phi}(\cdot))$ is sorted.

Proposition 8 (See Proof and Associated Algorithms in [3]): If $\mathbf{\Phi}$ sorts x and $\mathbf{\Psi}$ sorts t, then $\mathbf{\Phi}\circ\mathbf{\Psi}^{-1}$, where $\circ$ denotes function composition, matches x to t.

Let t_1, t_2 be any two target signals. If we can find a permutation Ψ such that $t_1(\mathbf{k}) = t_2(\mathbf{\Psi}(\mathbf{k}))$, then it is clear that

$$\begin{aligned}&\sum_{\mathbf{k}\in Q}(x(\mathbf{\Phi}(\mathbf{k}))-t_1(\mathbf{k}))^2\\ &\quad=\sum_{\mathbf{k}\in Q}(x(\mathbf{\Phi}(\mathbf{k}))-t_2(\mathbf{\Psi}(\mathbf{k})))^2 \qquad (9)\\ &\quad=\sum_{\mathbf{k}\in Q}(x(\mathbf{\Phi}\circ\mathbf{\Psi}^{-1}(\mathbf{k}))-t_2(\mathbf{k}))^2. \qquad (10)\end{aligned}$$

Therefore, finding a permutation that minimizes (9) for t_1 is equivalent to finding a permutation that minimizes (10) for t_2. Furthermore, it is clear that a permutation Ψ such that $t_1(\mathbf{k}) = t_2(\mathbf{\Psi}(\mathbf{k}))$ can be found iff t_1 and t_2 share the same distribution of values. Hence, signals that share the same distribution of values are equivalent and we are thus only concerned with identifying one member of each equivalent class. We describe these equivalence classes in Section IV.

If $\mathbf{\Phi}$ matches $x_o(\cdot)$ to a proper unidirectional T-periodic signal $t(\cdot)$, then we can interpret $\mathbf{\Phi}$ as analyzing $x_o(\cdot)$ into "percentiles" in the following way. Write $x(\cdot) = x_o(\mathbf{\Phi}(\cdot))$. Since $t(\cdot)$ is proper, $t(\cdot)$ has T distinct values, $t(0), t(1), \ldots, t(T-1)$. If $\nu \in \{0,\ldots,T-1\}$, then $t(n_1,\mathbf{n}') = t(\nu)$ if and only if $n_1 = \mu T+\nu$ for some $\mu \in \{0,1,\ldots,N/T-1\}$. If we arrange the values of $x_o(\cdot)$ in ascending order, with multiplicity, and divide this list of values into blocks of size N^M/T ("percentiles"), then the values in a single block will be those in the set

$$\{x(\mu T+\nu,\mathbf{n}') : 0 \le \mu \le N/T-1, \mathbf{n}' \in Q'\}$$

for some choice of $\nu \in \{0,\ldots,T-1\}$.

Proposition 9 (Invariance Property): Assume that $x_o(\cdot)$ and $y_o(\cdot)$ are signals on Q that share the same histogram of values. Let $t(\cdot)$ be a proper unidirectional T-periodic signal, and let $x(\cdot)$ and $y(\cdot)$ be permutations of $x_o(\cdot)$ and $y_o(\cdot)$ (respectively) that match $t(\cdot)$. Then, the DFT spectra of $x(\cdot)$ and $y(\cdot)$ satisfy

$$X(\mathbf{k}) = Y(\mathbf{k}) \quad \text{if } (N/T) \mid k_1 \quad \text{and} \quad \mathbf{k}' = \mathbf{0}. \tag{11}$$

Proof: Let $\alpha = k_1/(N/T)$. Then

$$\begin{aligned}X(k_1,\mathbf{0}) &= \frac{1}{K_{\mathbf{\Phi}}}\sum_{n_1=0}^{N-1}\sum_{\mathbf{n}'\in Q'} x(n_1,\mathbf{n}')\exp\left[-j\frac{2\pi}{N}k_1 n_1\right]\\ &= \frac{1}{K_{\mathbf{\Phi}}}\sum_{\nu=0}^{T-1}\sum_{\mu=0}^{N/T-1}\sum_{\mathbf{n}'\in Q} x(\mu T+\nu,\mathbf{n}')\\ &\quad\times\exp\left[-j\frac{2\pi}{N}k_1\nu\right]\exp\left[-j\frac{2\pi}{N}\alpha\mu\right]\\ &= \frac{1}{K_{\mathbf{\Phi}}}\sum_{\nu=0}^{T-1}\exp\left[-j\frac{2\pi}{N}k_1\nu\right]\\ &\quad\times\sum_{\mu=0}^{N/T-1}\sum_{\mathbf{n}'\in Q'} x(\mu T+\nu,\mathbf{n}').\end{aligned}$$

As we observed, since $t(\cdot)$ is proper unidirectional T-periodic, and since $x(\cdot)$ matches $t(\cdot)$, the double sum

$$\sum_{\mu=0}^{N/T-1}\sum_{\mathbf{n}'\in Q'} x(\mu T+\nu,\mathbf{n}')$$

is just the sum over one block of size N^M/T of values of $x_o(\cdot)$. Since $x_o(\cdot)$ and $y_o(\cdot)$ have the same histogram

$$\sum_{\mu=0}^{N/T-1}\sum_{\mathbf{n}'\in Q'} x(\mu T+\nu,\mathbf{n}') = \sum_{\mu=0}^{N/T-1}\sum_{\mathbf{n}'\in Q'} y(\mu T+\nu,\mathbf{n}') \tag{12}$$

and by reversing the steps above, we see that $X(k_1, \mathbf{0}) = Y(k_1, \mathbf{0})$. Q.E.D.

Remark 2 (Milder Conditions for Invariance): Note that the condition that $x_o(\cdot)$ and $y_o(\cdot)$ share the same histogram is actually stricter than required. By carefully examining the proof, one sees that $x_o(\cdot)$ and $y_o(\cdot)$ need only share the same averages over each of the analysis blocks [as given in (12)]. Furthermore, in this proposition, we only consider unidirectional signal as targets, but as will be proven in Theorem 2, signals that are not uni-directional are equivalent to uni-directional signals.

In fact, we can show that matched signals with the same histogram also share the entire FM spectra.

Proposition 10 (Invariance of Signal-Adaptive FM Spectra): Assume $x_o(\cdot)$ and $y_o(\cdot)$ are signals on Q that share the same histogram of values. Let $t(\cdot)$ be an arbitrary target signal, and let $\mathbf{\Psi}$ be a fixed permutation that sorts $t(\cdot)$. Let $x(\cdot)$, and $y(\cdot)$ be permutations of $x_o(\cdot)$ and $y_o(\cdot)$ (respectively) that match $t(\cdot)$. Then, the DFT spectra of $x(\cdot)$ and $y(\cdot)$ are the same. The reverse is also, clearly true. If the DFT spectra of $x(\cdot)$ and $y(\cdot)$ are the same, then the original signals $x_o(\cdot)$ and $y_o(\cdot)$ share the same histogram of values.

Proof: Let $\mathbf{\Phi_1}$ sort $x_o(\cdot)$, and let $\mathbf{\Phi_2}$ sort $y_o(\cdot)$. Then, $x_o(\mathbf{\Phi_1}(\cdot))$ and $y_o(\mathbf{\Phi_2}(\cdot))$ are the sorted lists of the same collection of values. It follows that $x = x_o(\mathbf{\Phi_1} \circ \mathbf{\Psi}(\cdot))$ and $y = y_o(\mathbf{\Phi_2} \circ \mathbf{\Psi}(\cdot))$ are also the same and hence their DFT spectra are the same. Q.E.D.

The results of Propositions 9 and 10 relate to the implementation of FM transforms. In implementing FM transforms, just like JPEG, we break the given image into blocks. If the histograms of the values between two adjacent blocks are not very different then it makes sense to apply differential pulse code modulation (DPCM) encoding between the FM coefficients of adjacent blocks. In practice, the milder conditions of Proposition 9 (see Remark 2) were found to hold, and DPCM was only applied to the FM coefficients specified in (11). We will return to this point in Section VI.

IV. Equivalence of Target Signals

We have suggested that, because of their sparse spectra and invariance property, unidirectional periodic signals form a family of target signals well-suited to the signal-adaptive FM transform strategy. In [3], however, emphasis was placed on DFT basis signals as the ideal targets for energy compaction via permutation. In this section, we explore the relationship between DFT basis signals and unidirectional periodic signals from the perspective of the signal-adaptive FM transform strategy. We will define a suitable equivalence relation between (target) signals and see that all DFT basis signals are equivalent to proper unidirectional periodic signals. Furthermore, we will describe the equivalence classes of DFT basis signals under the relation. For any family of target signals, the number of equivalence classes is of interest since it is a measure of richness and descriptive power of signal-adaptive FM transforms that match to the target signals of the family. For these results, we will use basic concepts from group theory, which can be found in [8].

According to Proposition 8, matching is accomplished by sorting. Thus, two target signals that share the same histogram of values will be matched by the same set of input signals, although the matching for a given input signal may be accomplished by a different permutation. Two target signals share the same histogram of values if and only if they are themselves related by a permutation, and so we are led to the following definition of equivalence.

Definition 2 (Equivalence of Target Signals): Two target signals $t(\cdot)$ and $s(\cdot)$ on Q are *equivalent*, written $t(\cdot) \sim s(\cdot)$, if and only if there is a permutation $\mathbf{\Phi}$ of Q such that $t(\cdot) = s(\mathbf{\Phi}(\cdot))$.

Of course, equivalent target signals need not have the same DFT spectrum. From previous observations, it is easy to see that two proper unidirectional periodic signals are equivalent if and only if they have the same set of values, and hence the same period.

Now we address equivalence of DFT basis signals. Fix $W_N = \exp[j2\pi/N]$, a primitive, complex Nth root of unity. For each $\mathbf{k} \in Q$, there is a *DFT basis signal* $t_{\mathbf{k}}(\cdot)$ given by $t_{\mathbf{k}}(\mathbf{n}) = W_N^{\mathbf{k}\cdot\mathbf{n}}$. A DFT basis signal can be thought of as a group homomorphism in the following way. Let

$$G = \{ W_N^r \mid r = 1, \ldots, N \}.$$

G is the set of complex Nth roots of unity, and it is easy to see that G forms a group under complex multiplication. On the other hand, since we view $Q = (\mathcal{Z}/N)^M$, Q forms a group under vector addition $\bmod N$. Any DFT basis signal $t_{\mathbf{k}}(\cdot)$ is a function $Q \to G$, and the fact that $t_{\mathbf{k}}(\cdot)$ is a group homomorphism follows from the familiar property of exponents

$$\begin{aligned} t_{\mathbf{k}}(\mathbf{n}+\mathbf{m}) &= \exp\left[j\frac{2\pi}{N}(\mathbf{k}\cdot\mathbf{n} + \mathbf{k}\cdot\mathbf{m}) \right] \\ &= \exp\left[j\frac{2\pi}{N}\mathbf{k}\cdot\mathbf{n} \right] \exp\left[j\frac{2\pi}{N}\mathbf{k}\cdot\mathbf{m} \right] \\ &= t_{\mathbf{k}}(\mathbf{n}) t_{\mathbf{k}}(\mathbf{m}). \end{aligned} \tag{13}$$

Since $t_{\mathbf{k}}(\cdot)$ is a group homomorphism, it follows that any two values of $t_{\mathbf{k}}(\cdot)$ are assumed with the same multiplicity. This property is stated more precisely as follows. For $z \in G$, write

$$t_{\mathbf{k}}^{-1}(z) = \{ \mathbf{n} \in Q \,|\, t_{\mathbf{k}}(\mathbf{n}) = z \}. \tag{14}$$

Proposition 11 (Multiplicity of DFT Basis Signals): For $z, w \in G$, if $t_{\mathbf{k}}^{-1}(z)$ and $t_{\mathbf{k}}^{-1}(w)$ are both nonempty, then $t_{\mathbf{k}}^{-1}(z)$ and $t_{\mathbf{k}}^{-1}(w)$ have the same number of elements.

Proof: It suffices to give the proof when $w = 1$ because the general case then follows by transitivity. Suppose $\mathbf{n}, \mathbf{m} \in t_{\mathbf{k}}^{-1}(z)$, i.e., that $t_{\mathbf{k}}(\mathbf{n}) = t_{\mathbf{k}}(\mathbf{m}) = z$. Then $t_{\mathbf{k}}(\mathbf{m}-\mathbf{n}) = zz^{-1} = 1$, so that $\mathbf{m}-\mathbf{n} \in t_{\mathbf{k}}^{-1}(1)$. This shows that for any particular choice of $\mathbf{n} \in t_{\mathbf{k}}^{-1}(z)$, we have

$$t_{\mathbf{k}}^{-1}(z) = \left\{ \mathbf{n} + \mathbf{p} \,|\, \mathbf{p} \in t_{\mathbf{k}}^{-1}(1) \right\}.$$

Clearly, then, $t_{\mathbf{k}}^{-1}(z)$ has the same number of elements as $t_{\mathbf{k}}^{-1}(1)$. Q.E.D.

From the fact that $t_{\mathbf{k}}(\cdot)$ is a group homomorphism, it is easy to verify that the set of values

$$t_{\mathbf{k}}(Q) = \{ t_{\mathbf{k}}(\mathbf{n}) \,|\, \mathbf{n} \in Q \} \tag{15}$$

forms a subgroup of G. The subgroups of G are well known, and we briefly describe them now. For further details, see the discussion of cyclic groups in [8]. If $r \in \{1, \ldots, N\}$, write

$$G_r = \{ W_N^{rn} \mid n \in \mathcal{Z} \}. \tag{16}$$

It is easy to check that G_r is a subgroup of G. In fact, every subgroup of G is of the form G_r for some $r \in \{1, \ldots, N\}$. Furthermore, if $r, s \in \{1, \ldots, N\}$, then G_r is a subgroup of G_s if and only if $\gcd(s, N) \mid \gcd(r, N)$ (as can be easily verified). It follows that $G_r = G_s$ if and only if $\gcd(r, N) = \gcd(s, N)$. In particular

$$G_r = G_{\gcd(r,N)} \tag{17}$$

and so the subgroups of G are in one-to-one correspondence with the positive divisors of N. The number of elements in G_r is $N/\gcd(r, N)$.

Example 1: To illustrate the ideas above we describe the subgroups of G more explicitly when $N = 2^m$. This choice of N is of particular interest for implementation. The positive divisors of N are the numbers 2^p for $p = 0, 1, \ldots, m$. Thus, the subgroups of G are $G = G_1, G_2, G_4, \ldots, G_{N/4}, G_{N/2}, G_N = \{1\}$. Notice that these subgroups are all *nested*:

$$G = G_1 \supset G_2 \supset \cdots \supset G_{N/4} \supset G_{N/2} \supset G_N = \{1\}. \tag{18}$$

Proposition 12 (Set of Values of DFT Basis Signal): $t_{\mathbf{k}}(Q) = G_r$, where $r = \gcd(\mathbf{k}) \bmod N$. Here, we understand that $r \in \{1, \ldots, N\}$ and $\gcd(\mathbf{k}) = \gcd(k_1, k_2, \ldots, k_M)$.

Proof: Using a well-known property of gcd (given in [9, p. 10]), we can find $\mathbf{n} \in \mathcal{Z}^M$ such that $\gcd(\mathbf{k}) = \mathbf{n} \cdot \mathbf{k}$. Then $r = \mathbf{n} \cdot \mathbf{k} \bmod N$, and it follows that $W_N^r = t_{\mathbf{k}}(\mathbf{n})$. Therefore, $G_r \subseteq t_{\mathbf{k}}(Q)$. On the other hand, since r is equal to $\gcd(\mathbf{k}) \bmod N$, we can find an integer a such that $r + Na = \gcd(\mathbf{k})$. With $p_i = k_i/(r + Na)$, it follows that $\mathbf{k} = (r + Na)\mathbf{p}$, and so for any $\mathbf{m} \in Q$,

$$\mathbf{k} \cdot \mathbf{m} = (r + Na)\mathbf{p} \cdot \mathbf{m}.$$

Then

$$t_{\mathbf{k}}(\mathbf{m}) = W_N^{r(\mathbf{p}\cdot\mathbf{m})} \in G_r.$$

This implies that $t_{\mathbf{k}}(Q) \subseteq G_r$. Q.E.D.

According to Proposition 11, $t_{\mathbf{k}}(\cdot)$ assumes its values with uniform multiplicity. Proposition 12 implies that the set of values of $t_{\mathbf{k}}(\cdot)$ is equal to a subgroup G_r of G. The number of distinct values of $t_{\mathbf{k}}$ is $N/\gcd(r, N)$, a divisor of N. From these observations, it follows that $t_{\mathbf{k}}(\cdot)$ is equivalent to a proper unidirectional $(N/\gcd(r, N))$-periodic signal.

We can now characterize the equivalence classes of DFT basis signals.

Theorem 2 (Equivalence of DFT Basis Signals): For $\mathbf{k}, \mathbf{n} \in Q$, $t_{\mathbf{k}}(\cdot) \sim t_{\mathbf{n}}(\cdot)$ if and only if $\gcd(\mathbf{k}) = \gcd(\mathbf{n}) \bmod N$.

Proof: $t_{\mathbf{k}}(\cdot) \sim t_{\mathbf{n}}(\cdot)$ if and only if $t_{\mathbf{k}}(\cdot)$ and $t_{\mathbf{n}}(\cdot)$ have the same histogram of values. In view of Proposition 11, the histograms are the same if and only if the two signals have the same set of values, i.e., if and only if $t_{\mathbf{k}}(Q) = t_{\mathbf{n}}(Q)$. By Proposition 12, this last condition holds if and only if $\gcd(\mathbf{k}) = \gcd(\mathbf{n}) \bmod N$. Q.E.D.

Notice that Theorem 2 implies that the number of equivalence classes of DFT basis signals is no more t in Example 1. *In particular, the number of equivalence classes of DFT basis signals depends only on N, not on the dimension M of the hypercube.*

Now, for matching signals to targets, we need only consider the number of distinct elements in each target. This is due to the fact that all signal samples that get permuted to match the location of the same target sample are (from the perspective of the target) equivalent (also see our discussion of bucketing in [3]). Returning to Example 1, we note that for matching signals to targets, we observe that $G_{N/2}$ has two elements, $G_{N/4}$ has four elements , …, G_N has N elements. Thus, we need a single bit per signal sample for matching signals to the unique uni-directional signal with the same elements as $G_{N/2}$, two bits per signal sample for matching signals to the unique unidirectional signal with the same elements as $G_{N/4}, \ldots, \log_2(N)$ bits per signal sample for matching signals to the unique uni-directional signal with the same elements as G. This is summarized in Fig. 1. Furthermore, in Section V, we demonstrate how the matching can be achieved for two-dimensional images with uniformly distributed samples in two and four bins.

V. Examples of FM Transforms

In this section, we demonstrate the use of FM Transforms for two-dimensional images. We will present examples for images associated with $G_{N/2}$ and $G_{N/4}$. For $G_{N/2}$-examples, we use signals that have a histogram of two equally distributed values. For $G_{N/4}$-examples, we use signals that have a histogram of four equally distributed values. We will also address implementation issues.

Without loss of generality, we pick a 2-D signal that has a histogram with two equally distributed values. Consider

$$x = \begin{bmatrix} \overbrace{v_1 \quad v_1 \quad \ldots, \quad v_1}^{\text{N/2 samples}} & \overbrace{v_2 \quad v_2 \quad \ldots, \quad v_2}^{\text{N/2 samples}} \\ \vdots & \vdots \\ v_1 \quad v_1 \quad \ldots, \quad v_1 & v_2 \quad v_2 \quad \ldots, \quad v_2 \end{bmatrix}, \quad v_1 > v_2.$$

For each sample, we want to assign a single bit to indicate which bin the sample falls in

$$C = \begin{bmatrix} \overbrace{0 \quad 0 \quad \cdots \quad 0}^{\text{N/2 samples}} & \overbrace{1 \quad 1 \quad \cdots \quad 1}^{\text{N/2 samples}} \\ \vdots & \vdots \\ 0 \quad 0 \quad \cdots \quad 0 & 1 \quad 1 \quad \cdots \quad 1 \end{bmatrix}.$$

Using the bit codes in C, we can re-arrange the samples in the original signal so as to match the appropriate transform domain samples. We match samples by mapping the smallest signal value to the smallest transform domain value, and then the next smallest signal value to the next smallest transform domain value and so on. For this two-bin signal, the most appropriate FFT basis function is

$$[\exp j\pi n_1]_{0 \le n_1, n_2 \le N-1} = \begin{bmatrix} 1 & -1 & 1 & -1 & \cdots & 1 & -1 \\ \vdots & \vdots & \vdots & \vdots & \vdots & \vdots & \vdots \\ 1 & -1 & 1 & -1 & \cdots & 1 & -1 \end{bmatrix}.$$

Number of bins in the histogram	*Associated Subgroups*	*Permutation bits per sample*	*AM-FM Spectrum Coefficients (plus DC coefficient)*
$T = 2$	$G_{N/2}$	1 bps	$1 + 1$
$T = 4$	$G_{N/2} \subset G_{N/4}$	2 bps	$2 + 1$
$T = 8$	$G_{N/2} \subset G_{N/4} \subset G_{N/8}$	3 bps	$3 + 1$
$\vdots$	$\vdots$	$\vdots$	$\vdots$
$T = N/2$	$G_{N/2} \subset G_{N/4}$ $\cdots \subset G_2$	$\log_2(N) - 1$ bps	$\log_2(N) - 1 + 1$
$T = N$	$G_{N/2} \subset G_{N/4}$ $\cdots \subset G_2 \subset G$	$\log_2(N)$ bps	N

Fig. 1. Relationships between FFT subgroups and discrete signals with uniformly distributed samples. The required bits per sample denote the number of bits that are required for encoding the permutation for the FM transform. The FM spectrum coefficients are described in Proposition 6. Also, examples of FM transforms for the cases $T = 2$ and $T = 4$ are described in Sections V and VI.

Using the bit codes C, we map the original signal x so as to match this basis function. For the permuted signal x_P, we write

$$x_P = \begin{bmatrix} v_1 & v_2 & v_1 & v_2 & \cdots & v_1 & v_2 \\ \vdots & \vdots & \vdots & \vdots & \vdots & \vdots & \vdots \\ v_1 & v_2 & v_1 & v_2 & \cdots & v_1 & v_2 \end{bmatrix}. \tag{19}$$

We note that x_P has a period of two along the horizontal coordinate. Hence, x_P is a 2-D example of a unidirectional, period-2 signal. Along the vertical coordinate, x_P remains constant.

We next write the permuted signal as

$$x_P = \frac{1}{2}(v_1 + v_2) \begin{bmatrix} 1 & 1 & 1 & 1 & \cdots & 1 & 1 \\ \vdots & \vdots & \vdots & \vdots & \vdots & \vdots & \vdots \\ 1 & 1 & 1 & 1 & \cdots & 1 & 1 \end{bmatrix} + \frac{1}{2}(v_1 - v_2) \begin{bmatrix} 1 & -1 & 1 & -1 & \cdots & 1 & -1 \\ \vdots & \vdots & \vdots & \vdots & \vdots & \vdots & \vdots \\ 1 & -1 & 1 & -1 & \cdots & 1 & -1 \end{bmatrix}. \tag{20}$$

The FM spectrum for this example is nothing but the FFT of the permuted signal. As shown in (20), the permuted signal requires two coefficients. This example illustrates a simple application of Proposition 6.

A numerical 1-D example is shown in Fig. 2. In this example, the FM transform can reconstruct the signal exactly using 1.04 bits per sample. The FM transform is exact since the FM spectral coefficients are computed after multiplying by the two roots of unity: 1 and -1 (which can be represented exactly).

Next, we examine signals that have a histogram of four equally distributed values. Without loss of generality, we pick a simple member of this general class of signals (see (21), shown at the bottom of the next page), satisfying $v_1 > v_2 > v_3 > v_4$. We encode the permutation required to match the signal to the FFT basis functions shown in (22) at the bottom of the page. For this signal, we look for FFT basis functions that have period 4 in the horizontal direction. Note that both $[\exp j\pi n_1]_{0 \le n_1, n_2 \le N-1}$ and $[\exp j(\pi/2)n_1]_{0 \le n_1, n_2 \le N-1}$ are such basis functions. This observation motivates the subgroup property described in Fig. 1. The subgroup property stems from the fact that period

$$x = \begin{bmatrix} \overbrace{v_1 \ v_1 \ \cdots \ v_1}^{\text{N/4 samples}} & \overbrace{v_2 \ v_2 \ \cdots \ v_2}^{\text{N/4 samples}} & \overbrace{v_3 \ v_3 \ \cdots \ v_3}^{\text{N/4 samples}} & \overbrace{v_4 \ v_4 \ \cdots \ v_4}^{\text{N/4 samples}} \\ \vdots & \vdots & & \\ \underbrace{v_1 \ v_1 \ \cdots \ v_1}_{\text{N/4 samples}} & \underbrace{v_2 \ v_2 \ \cdots \ v_2}_{\text{N/4 samples}} & \underbrace{v_3 \ v_3 \ \cdots \ v_3}_{\text{N/4 samples}} & \underbrace{v_4 \ v_4 \ \cdots \ v_4}_{\text{N/4 samples}} \end{bmatrix} \tag{21}$$

$$C = \begin{bmatrix} \overbrace{0 \ 0 \ \cdots \ 0}^{\text{N/4 samples}} & \overbrace{1 \ 1 \ \cdots \ 1}^{\text{N/4 samples}} & \overbrace{2 \ 2 \ \cdots \ 2}^{\text{N/4 samples}} & \overbrace{3 \ 3 \ \cdots \ 3}^{\text{N/4 samples}} \\ \vdots & \vdots & & \\ \underbrace{0 \ 0 \ \cdots \ 0}_{\text{N/4 samples}} & \underbrace{1 \ 1 \ \cdots \ 1}_{\text{N/4 samples}} & \underbrace{2 \ 2 \ \cdots \ 2}_{\text{N/4 samples}} & \underbrace{3 \ 3 \ \cdots \ 3}_{\text{N/4 samples}} \end{bmatrix} \tag{22}$$

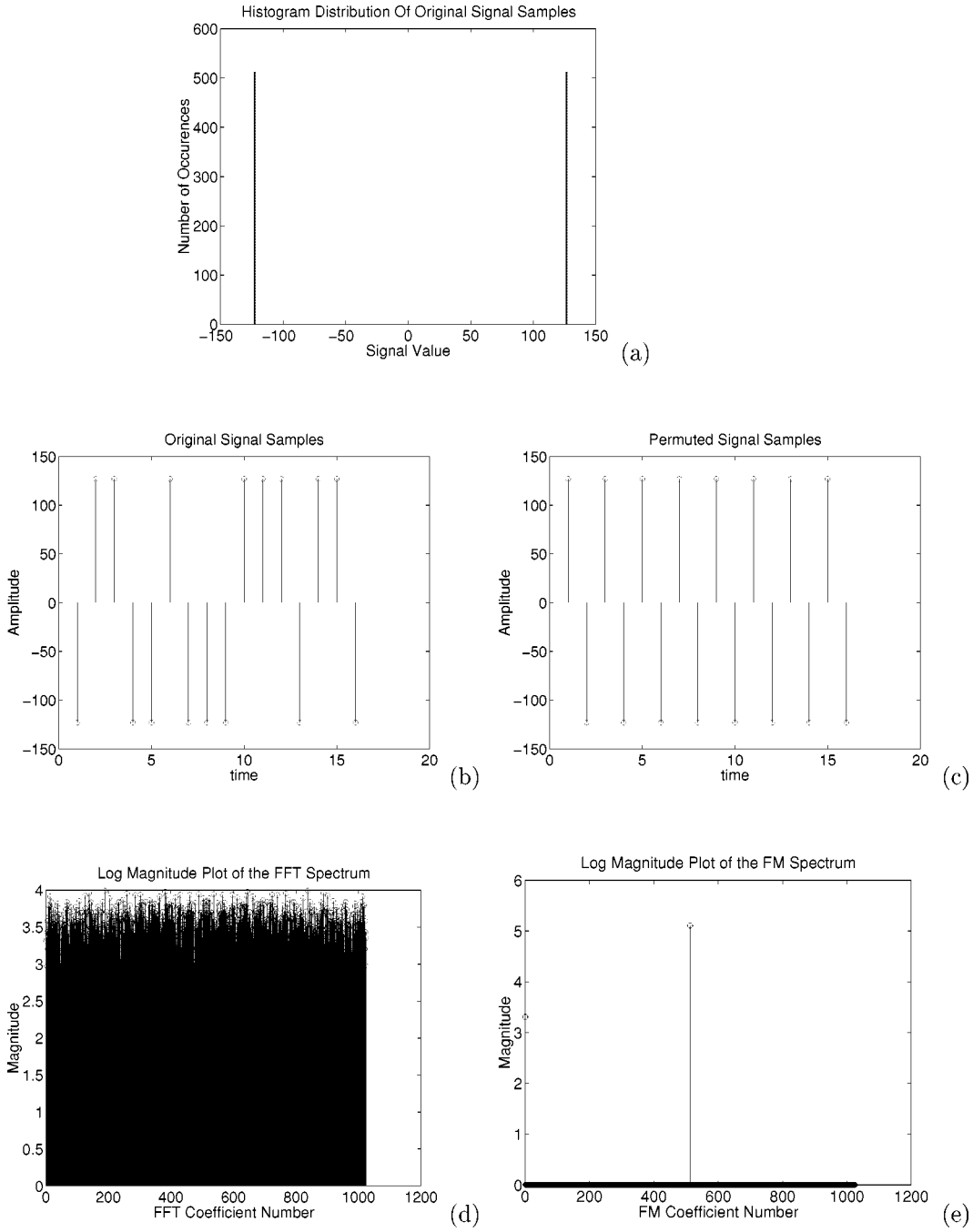

Fig. 2. DFT and FM Spectrum results for a signal that is uniformly distributed in two bins (127 and -123). In (a), we show the histogram of the signal. In (b), we show the first 16 samples of the signal (out of a total of 1024 samples), and its DFT magnitude spectrum in (d). In (c), we show the first 16 samples of the permuted signal, and its corresponding, FM spectrum in (e). The entropy of the DFT coefficients is 17.89 bits per sample, and the PSNR is 86 dB. The FM spectrum and permutation bits correspond to 1.04 bits per sample, and the PSNR is infinite.

T signals are also of period $2T, 4T, 8T, \ldots$. Now, to match our signal to the FFT basis functions: $[\exp j\pi n_1]_{0\leq n_1,n_2\leq N-1}$ and $[\exp j(\pi/2)n_1]_{0\leq n_1,n_2\leq N-1}$, we use the bit codes C to re-arrange x into a period 4 signal

$$x_P = \begin{bmatrix} v_1 & v_2 & v_3 & v_4 & \cdots & v_1 & v_2 & v_3 & v_4 \\ \vdots & \vdots & \vdots & \vdots & \vdots & \vdots & \vdots & \vdots & \vdots \\ v_1 & v_2 & v_3 & v_4 & \cdots & v_1 & v_2 & v_3 & v_4 \end{bmatrix} \quad (23)$$

The FM spectrum is the FFT spectrum of the permuted signal x_P. As discussed earlier, it is captured in the coefficients of $[\exp j\pi n_1]_{0\leq n_1,n_2\leq N-1}$, $[\exp j(\pi/2)n_1]_{0\leq n_1,n_2\leq N-1}$, and the dc coefficient.

A numerical, 1-D example is shown in Fig. 3. The FM transform can reconstruct the signal exactly using 2.07 bits per sample. The FM transform is exact since the FM spectral coefficients are computed after multiplying by the four roots of unity: 1, -1, $\sqrt{-1}$, $-\sqrt{-1}$ (which can be represented exactly).

It is clear how to extend our discussion to $8, 16, \ldots, N$ bins. Furthermore, it is fairly clear that the dimensionality of the signal x does not affect our ability to rearrange the samples

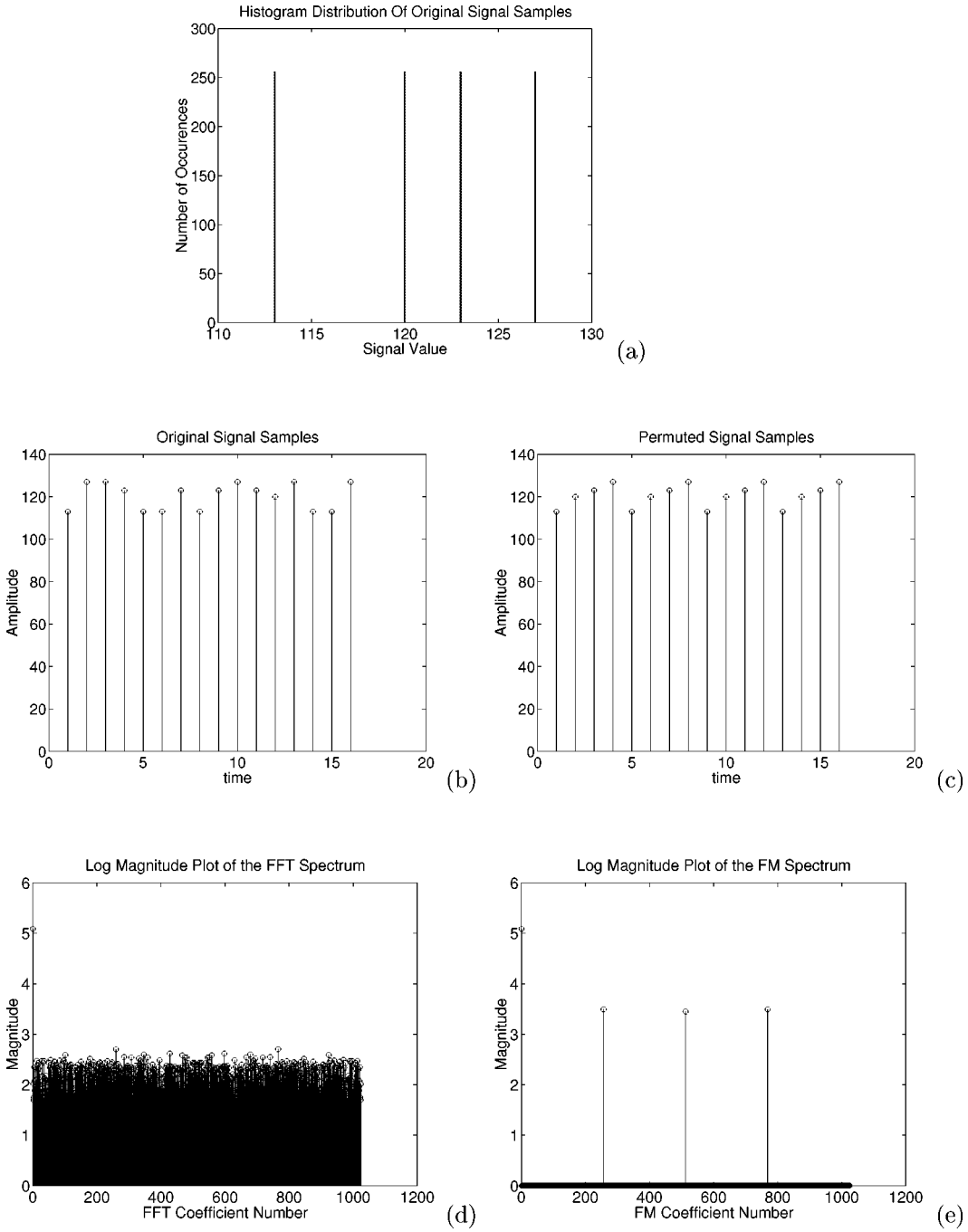

Fig. 3. DFT and FM Spectrum results for a signal that is uniformly distributed in four bins (113, 120, 123, and 127). The figures are the same as in Fig. 2. The entropy of the DFT coefficients is 16.03 bits per sample, and the PSNR is 86 dB. The FM spectrum and permutation bits correspond to 2.07 bits per sample, and the PSNR is infinite.

along a single dimension. In our examples, we chose the n_1-coordinate.

For the DCT, we look for permutations that produce signals with twice the period of the corresponding FFT group. This is accomplished by mirroring the samples within the period. We illustrate this approach for the two-bin case

$$x_P = \begin{bmatrix} v_1 & v_2 & v_2 & v_1 & \cdots & v_1 & v_2 & v_2 & v_1 \\ \vdots & \vdots & \vdots & \vdots & \vdots & \vdots & \vdots & \vdots & \vdots \\ v_1 & v_2 & v_2 & v_1 & \cdots & v_1 & v_2 & v_2 & v_1 \end{bmatrix} \quad (24)$$

and the four-bin case

$$x_P = \begin{bmatrix} v_1 & v_2 & v_3 & v_4 & v_4 & v_3 & v_2 & v_1 & \cdots \\ \vdots & \vdots & \vdots & \vdots & \vdots & \vdots & \vdots & \vdots & \vdots \\ v_1 & v_2 & v_3 & v_4 & v_4 & v_3 & v_2 & v_1 & \cdots \end{bmatrix}. \quad (25)$$

To be able to visually identify how the permuted images look like, we examine (24) and (25) as digital images. For (24), we assign the black color for v_1, and the white color for v_2. Along each column of this image, the intensity remains constant. The image appears as an alternating sequence of black and white

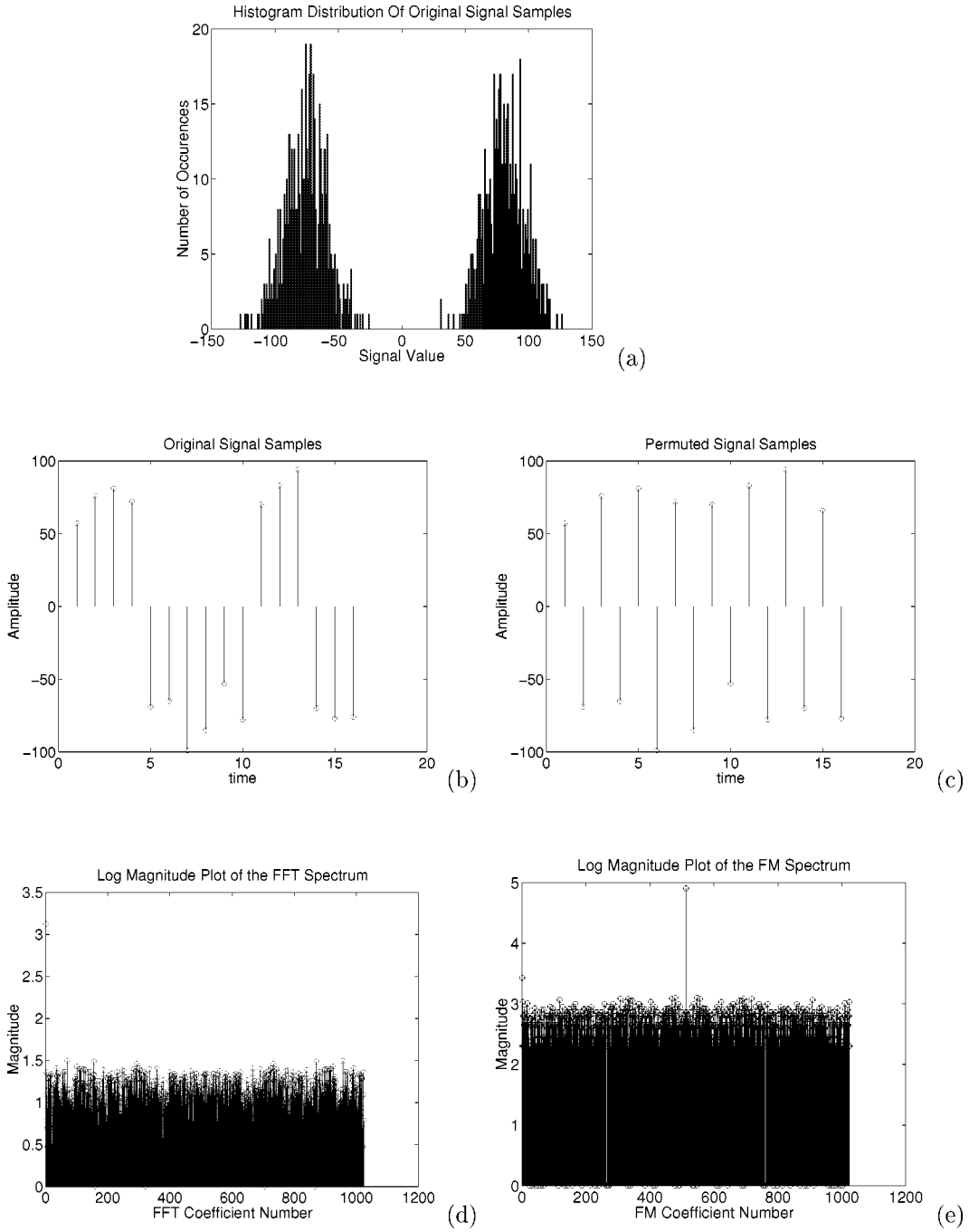

Fig. 4. DFT and FM Spectrum results for a signal that is normally distributed in two bins. The figures are the same as in Fig. 2. For the DFT, the ac coefficients were divided by 200 before rounding of to the nearest integer values. The dc coefficient was divided by 2 before rounding to the nearest integer value. Similary, for the FM transform, the spectral coefficients that did not capture the energy were rounded in the same way [see text and (e)]. The entropy of the DFT coefficients is 10.3 bits per sample, and the PSNR is 39.9 dB. The FM spectrum and permutation bits correspond to 6.8 bits per sample, and the PSNR is 40.1 dB.

stripes. Each stripe is two pixels thick. Similarly, (25) appears as an alternating sequence of white, two-pixel columns (coming from columns of v_1, v_1) and black, two-pixel columns (coming from columns of v_4, v_4). Between the white and black stripes, we have a transition stripe coming from columns of v_2, v_3. We expect to observe similar stripe patterns when examining general images permuted to match the structures of (24) and (25). This is seen in Fig. 8(a) and (b), the permuted blocks of Fig. 12(a) and (b), (see Section VI for more details).

We generalize our discussion for matching any given signal to $[\exp j\pi n_1]_{0\le n_1,n_2\le N-1}$, or $[\exp j(\pi/2)n_1]_{0\le n_1,n_2\le N-1}$. For matching a signal to $[\exp j\pi n_1]_{0\le n_1,n_2\le N-1}$, we simply permute the lowest half of the samples as if they were v_1, while samples in the upper half are permuted as v_2

$$\overbrace{x_1 \le x_2 \le \cdots \le x_{N^2/2}}^{\text{permuted as } v_2} \le \overbrace{x_{N^2/2+1} \le x_{N^2/2+2} \le \cdots \le x_{N^2}}^{\text{permuted as } v_1}. \tag{26}$$

For matching a signal to $[\exp j(\pi/2)n_1]_{0\le n_1,n_2\le N-1}$, we break

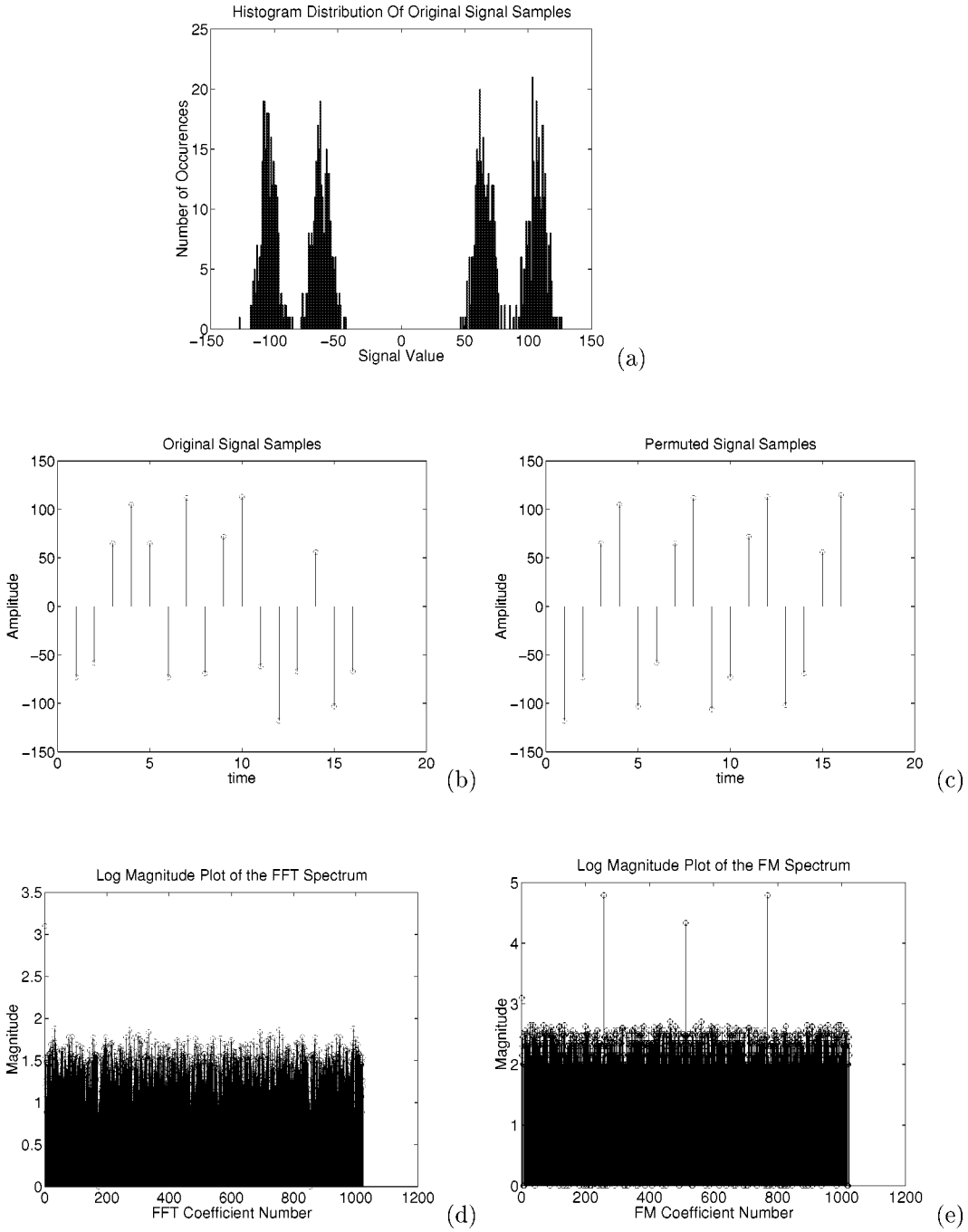

Fig. 5. DFT and FM spectrum results for a signal that is normally distributed in four bins. The figures are the same as in Fig. 2. For the DFT, the ac coefficients were divided by 100 before rounding of to the closest integer values. Similary, for the FM transform, the spectral coefficients that did not capture the energy were rounded in the same way [see text and (e)]. The entropy of the DFT coefficients is 12.4 bits per sample, and the PSNR is 45.9 dB. The FM spectrum and permutation bits correspond to 7.3 bits per sample, and the PSNR is 46.2 dB.

the signal into quartiles

$$\overbrace{x_1 \le x_2 \le \cdots \le x_{N^2/4}}^{\text{permuted as } v_4} \le \overbrace{x_{N^2/4+1} \le x_{N^2/4+2} \le \cdots \le x_{N^2/2}}^{\text{permuted as } v_3} \le \cdots \le \overbrace{x_{3N^2/4+1} \le x_{3N^2/4+2} \le \cdots \le x_{N^2}}^{\text{permuted as } v_1}. \quad (27)$$

Numerical results are presented in Figs. 4 and 5. In these examples, two multi-modal, normally distributed signals are used. In the first example, the FM reconstructed signal has slightly less distortion at less than 70% the bit rate of the corresponding discrete Fourier transform. Similarly, for the second example, the FM reconstructed signal has slightly less distortion at less than 60% the bit rate of the corresponding discrete Fourier transform.

Using this general method for matching arbitrary signals to $[\exp j\pi n_1]_{0\le n_1,n_2\le N-1}$, and $[\exp j(\pi/2)n_1]_{0\le n_1,n_2\le N-1}$, we conjecture that most of the signal energy should be captured in (i) the ideal FM coefficients described in Proposition 6, followed by (ii) the horizontal FM coefficients, and (iii) the nonhorizontal FM coefficients. The claim that the ideal FM coefficients capture most of signal energy is vividly demonstrated in the exam-

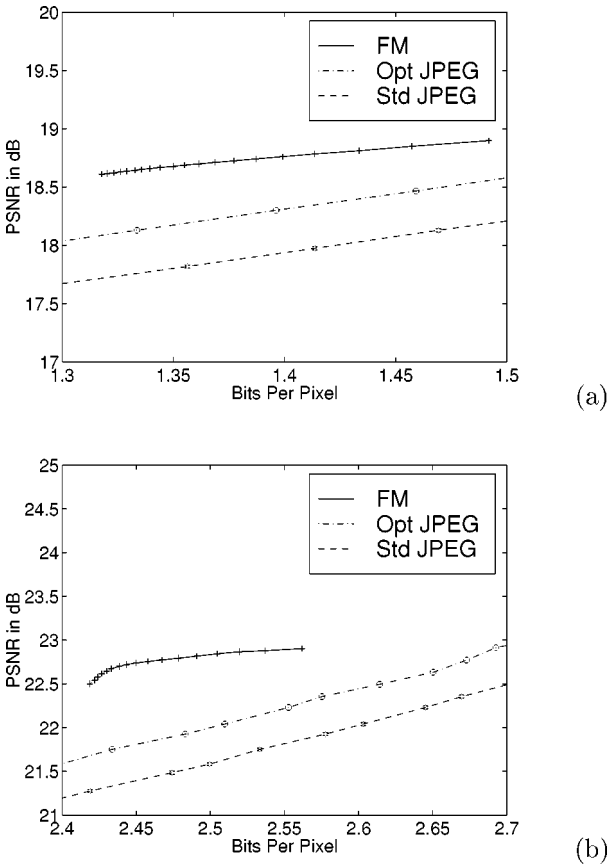

Fig. 6. Rate-distortion curves for FM transform and JPEG for the sensor image. In all plots, we plot the PSNR versus bits per pixel. The FM-transform results are plotted in solid line, while JPEG results are plotted using a dashed line. In (a), we show results for one-bit permutations. In (b), we show results for two-bit permutations.

ples of Figs. 2(d), 2(e), 3(d), 3(e), 4(d), (e), and 5(d) and 5(e). The ideal FM coefficients are above all other coefficients in orders of magnitude. The claim that the horizontal FM coefficients are expected to capture more of the energy than the nonhorizontal FM coefficients is less obvious. To see why this is true, we return to the permuted matrices of (19), (23), (24), and (25). We recall that the permuted images are formed after first sorting the image values, and then arranging successive pixels across a column. Hence, we expect far less intensity variation across a column than across a row. This conjecture is also seen to hold for more general images [see the permuted images of Fig. 8(a), (b), and the permuted blocks of Fig. 12(a) and (b)]. We observe far less intensity variations across the columns than across the rows. In the ideal case, when there is no intensity variation along the columns of an image, the nonhorizontal Spectral coefficients are zero. It then follows that the horizontal spectral coefficients capture more of the energy in the image.

VI. Applications

As a sample application of the discrete FM transform, we consider a natural and significant example: signal compression. Consider the original images displayed in Fig. 7(a)[1] and Fig. 11(a) (a 256×256 grayscale image). The two examples that

[1]This is a 256×256 image segment of the sensor image `m78p1f24hh.884`, and it was taken from http://www.mbvlab.wpafb.af.mil/public/MBVDATA/adts.htm.

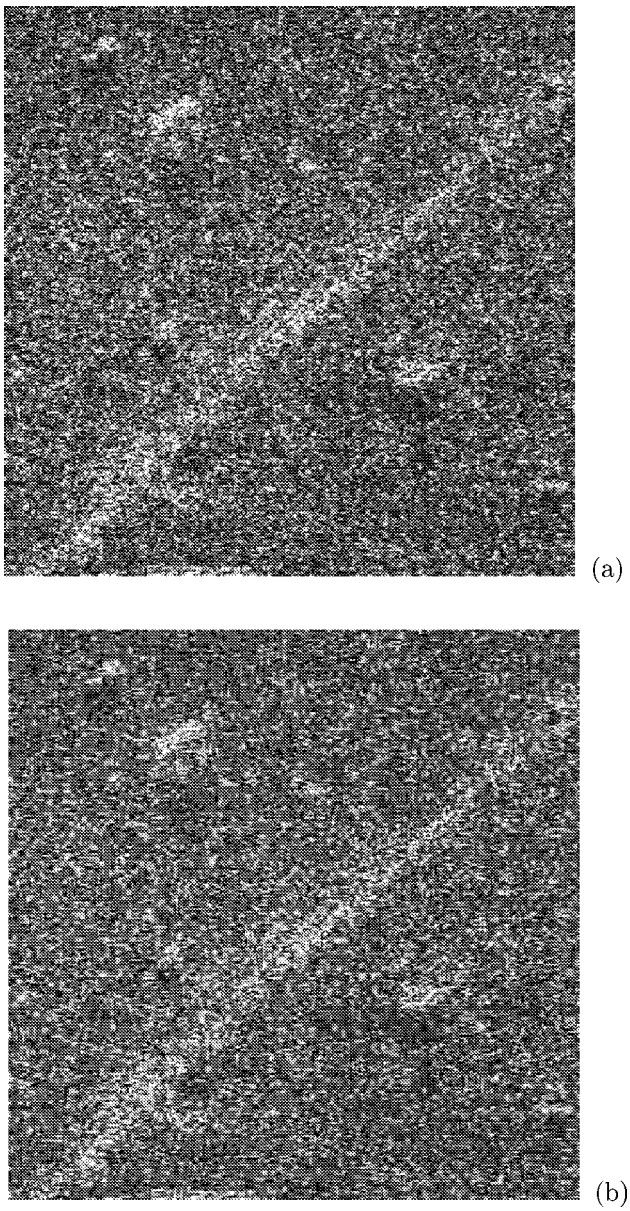

Fig. 7. JPEG results for the sensor image. (a) The original image is an 8-bit image of size 256×256. The optimized JPEG reconstructed image is shown in (b). The optimized JPEG is computed at 1.33 bits per pixel at a quality factor of 20, at a PSNR of 18.13 dB.

we are showing are well suited for the FM transform methods that we have developed, essentially due to the noiselike texture that they contain. JPEG and most traditional techniques have not being very effective in compressing these kinds of textures.

To efficiently capture the textures in the two examples, we implement two distinct transforms 1) FM transforms on 8×8 blocks and 2) a hybrid technique using either an FM transform or the DCT on each 8×8 block. For the sensor image, the same texture is present throughout the image, and we applied the FM transform on each 8×8 block (see results in Fig. 6). For the Mandrill image, the texture is only found on portions of the image, and we thus applied the hybrid transform, in an attempt to allow the FM transform technique to effectively capture the texture, while leaving the smooth regions to the DCT. For general images, where there is no knowledge of the presense of texture in the image, the hybrid method is clearly the best one to try.

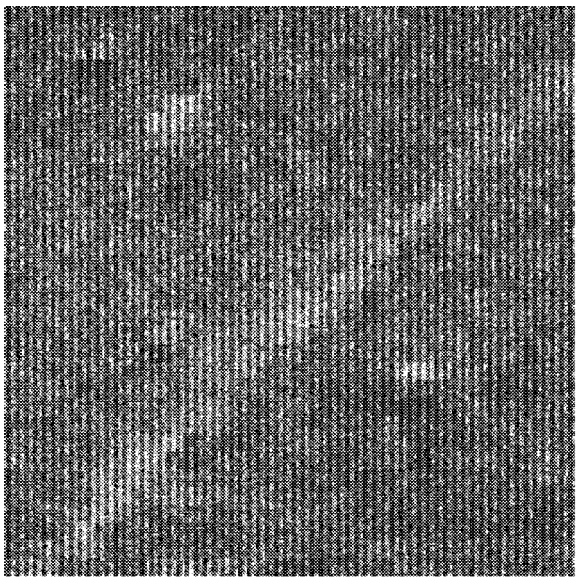

(a)

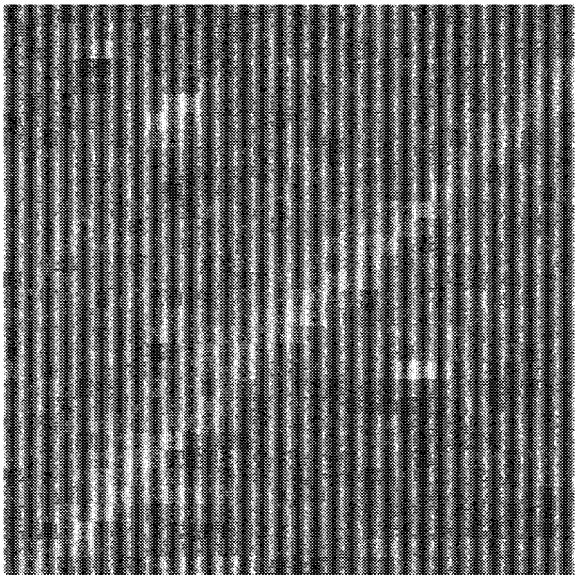

(b)

Fig. 8. Permuted images for the sensor example. (a) The one-bit permutation image and (b) the two-bit permutation image.

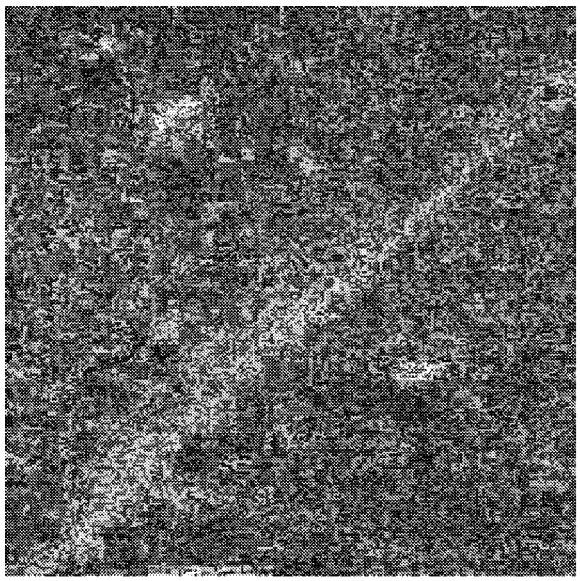

(a)

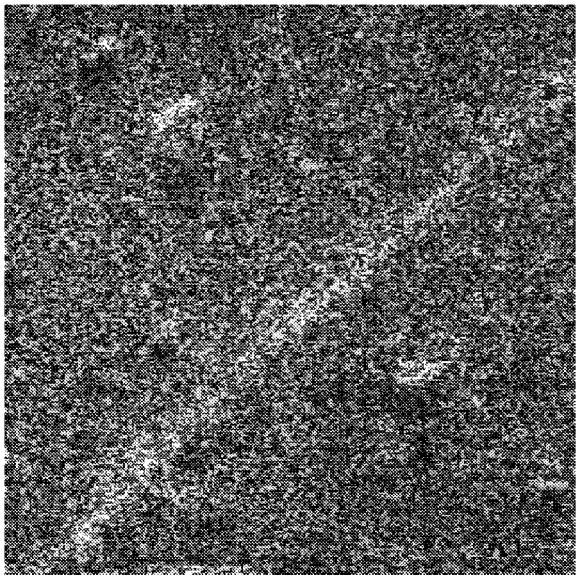

(b)

Fig. 9. FM reconstructed images for the sensor example. In (a), we have the reconstructed image for the single bit FM transform. It is encoded at 1.49 bit per pixel, with a PSNR of 18.90 dB. In (b), we have the reconstructed image for the two-bit FM transform. It is encoded at 2.42 bits per pixel, with a PSNR of 22.50 dB.

To analyze the performance of the FM transforms, we consider the permutation overhead. We only consider target signals that have a constant overhead of either one bit per sample, or an overhead of two bits per sample (as we have described in Section V). To reduce the permutation overhead, we employ two different methods for encoding the permutation bits. In direct encoding, we simply store the bit codes without processing. For the images that we consider here, this is the preferred method. In scanned encoding, we scan the 8×8 array of codes in horizontal, vertical or some other scan order. The scanning direction is defined to be orthogonal to the direction of maximum energy in the two-dimensional power spectrum. For example, if the sum of all the power along the diagonal frequencies $(f_1 = f_2)$ is greater than the sums along the horizontal and vertical directions, we use zig-zag scanning of the permutation codes. For the images that we are presenting here, there is usually no preferred direction and there is no real need to determine the preferred direction. However, for applying FM transforms to smooth images, for future research, we hope that scanning codes will prove useful.

It is clear that all coding gains are due to the quantization of the FM spectrum. For a specified number of permutation bits per sample, we have a corresponding number of dominant FM coefficients: the nonzero spectrum coefficients of the unidirectional $T|N$-periodic signal (see definition in Proposition 1). For theDCT implementation of the FM transform, the dominant coefficients are a bit different. It is easy to show that in the two-dimensional DCT-spectrum, in the first row, the dominant coefficients are the 0th and 4th coefficients for one-bit permutations, and they are the 0th, 1st, 3rd, 5th and 7th coefficients for two-bit permutations. Due to the invariance of these dominant FM coefficients (see Proposition 9), we apply a DPCM technique to encode these coefficients (similar to the

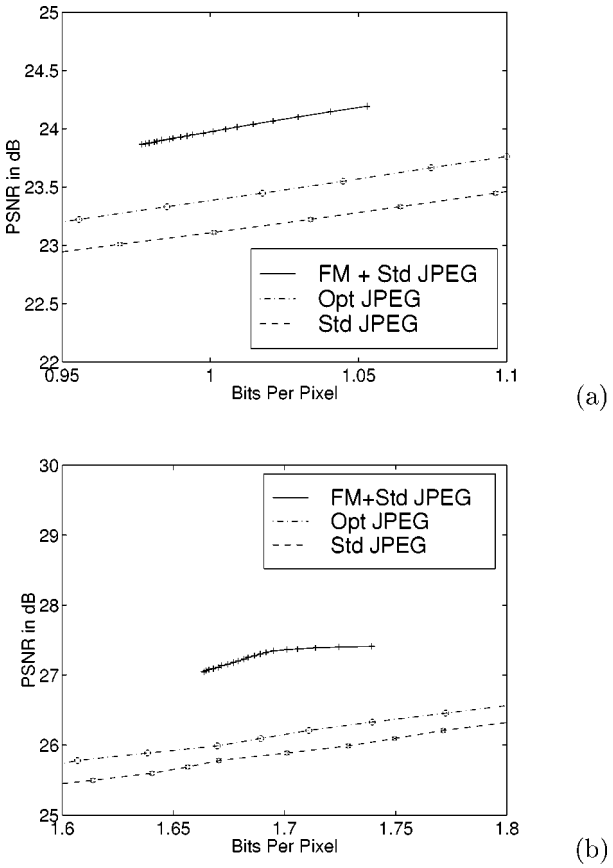

Fig. 10. Rate-distortion results for the Mandrill image. For this image, we used a hybrid transform (see text). For one-bit permutations, we show the results in (a). For two-bit permutations, we show the results in (b). The solid lines represent the hybrid FM transform, while the dashed lines represent JPEG.

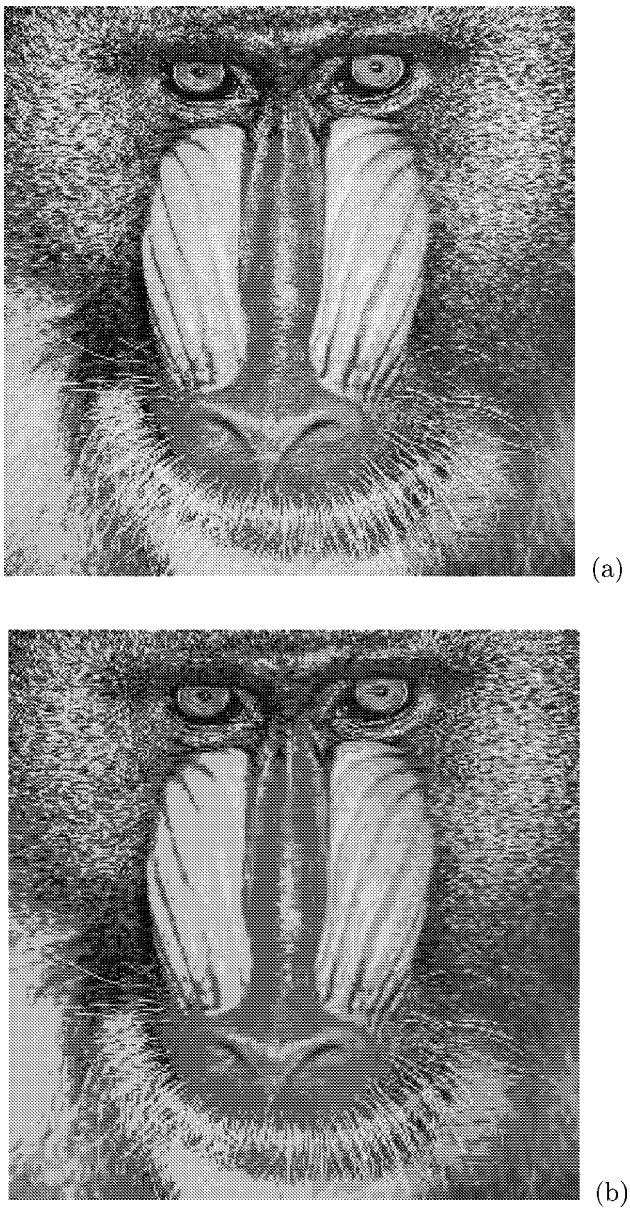

Fig. 11. Mandrill image results for JPEG. In (a), we show the original Mandrill image. In (b), we show the (optimized) JPEG image for the quality set to 30 in `cjpeg`. At this quality level, JPEG is coded at 1.0745 bits per sample, at a PSNR of 23.67 dB.

DPCM of the dc coefficient in JPEG). Furthermore, we used the standard Huffman table for encoding dc coefficients for encoding these coefficients (given in [10]).

The permuted images are shown in Figs. 8 and 12, where we plot the permuted images corresponding to Figs. 7(a) and 11(a). The horizontal stripes in the permuted images confirm our expectation that for the noiselike, granular textured regions, suitable permutations have converted them into almost unidirectional, periodic signals (see Section V). Most promising is the fact that FM reconstructed images shown in Figs. 9 and 13 are free from blocking artifacts that are clearly present in the JPEG images of Figs. 7(b) and 11(b). Blocking artifacts have been eliminated due to 1) the permuted image blocks are approximately unidirectional periodic, and since unidirectional periodic signals are free of any blocking artifacts, the permuted image blocks can be encoded with less blocking artifacts, and 2) the reduced artifacts in the permuted image blocks are eliminated when the image samples at the edges are permuted to different locations within each block. It is easy to recognize what an FM image will look like at very low bit rates. In the extreme case, where only the dominant FM coefficients are kept, the low-bit rate FM image appears like a histogram equalized version of the original image (equalized over each block). The number of equalization levels is determined by the number of permutation bits.

Based on our discussion on the relative importance of different coefficients, it is natural to chose different quantization levels based on the importance of each coefficient. To specify the quantization levels, we use three different quality factors: (i) *iq* for ideal quality factor, which is used with the horizontal, unidirectional periodic coefficients, (ii) *hq* for horizontal quality factor, which will is used for the horizontal coefficients that are not covered by the ideal quality factor *iq*, and (iii) *nhq* for nonhorizontal quality factors, which is used for the nonhorizontal coefficients. We use very simple relationships for describing the relationships among the quality factors. For one-bit permutations, we set $hq = 4iq$ and $nhq = 4iq$, while for two-bit permutations, we set $hq = 2iq$ and $nhq = 2hq$. Hence, given a value for the ideal-quality factor *iq*, we obtain simple expressions for *hq* and *nhq*, which we can use to compute the quantization levels for: (i) $iql(\cdot)$ for the ideal quantization levels corresponding to *iq*, (ii) $hql(\cdot)$ for the horizontal quantization levels corresponding *hq*, (iii) $nhql(\cdot)$ for the nonhorizontal quantization levels corresponding to *hq*. Again, we use simple, empirical

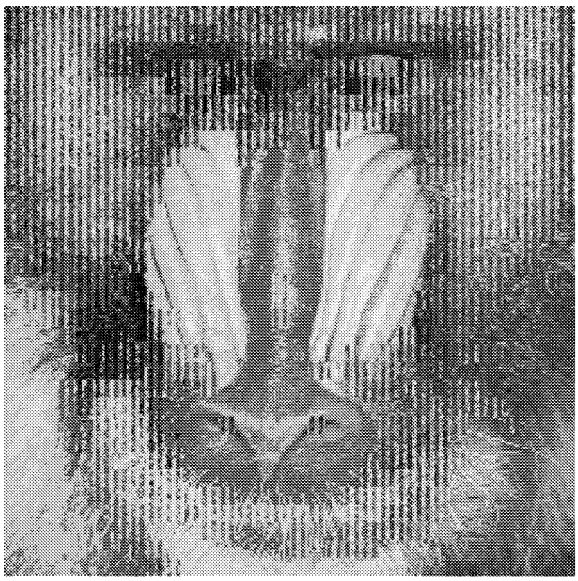

(a)

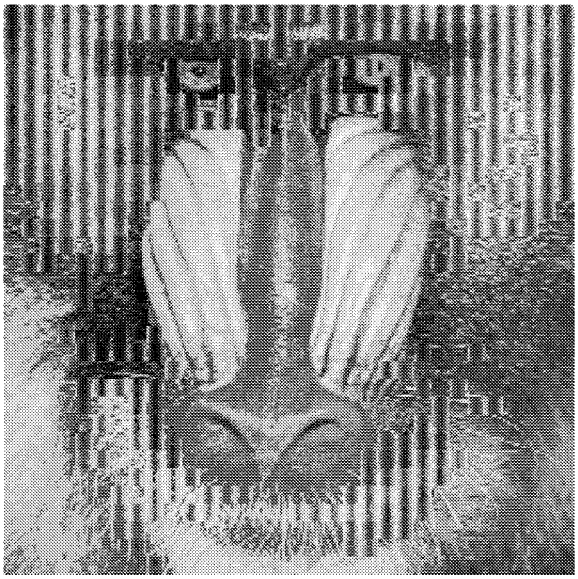

(b)

Fig. 12. Permutation images for the Mandrill example. The one-bit permuted image is shown in (a), while in (b), we show the two-bit permuted image. When the image does not appear permuted, we are using JPEG for that block.

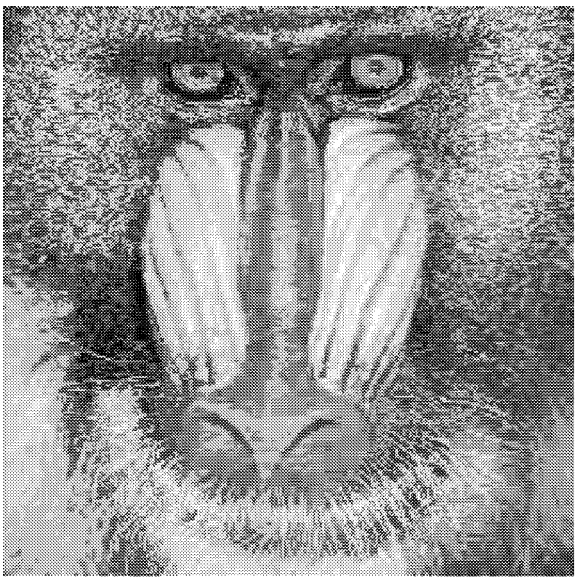

(a)

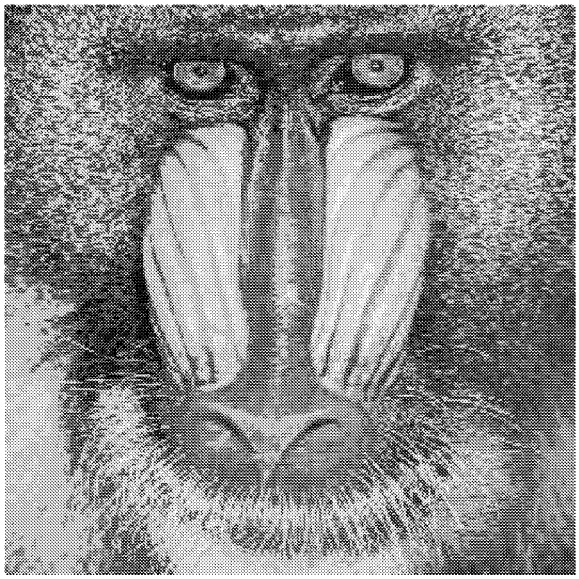

(b)

Fig. 13. FM reconstruction results for the Mandrill image. For one-bit permutations, we show the reconstructed image in (a). It is compressed at 1.49 bit per pixel, with a PSNR of 18.90 dB. Similarly, for two-bit permutations, we show the results in (b). It is compressed at 2.42 bits per pixel, with a PSNR of 22.50 dB.

expressions (for the standard 8×8 image block)

$$\begin{aligned} iql(n) &= 1 + (1+n)iq \\ hql(m) &= 1 + (1+m)hq \\ nhql(i-1,j) &= 1 + (1+i+j)nhq. \end{aligned} \tag{28}$$

Now that we have specified the quantization levels for the FM transform alone, we turn to the problem of implementing a hybrid transform. For the hybrid transform, we would like to specify the DCT quantization tables so that the number of bits required for encoding DCT blocks and the number of bits required for encoding FM blocks are comparable. For using hybrid transforms to compress images at about two bits per sample, we use the standard quantization table of the DCT [10]. For using hybrid transforms to compress images at one bit per sample, we multiply each entry in the quantization table by two and use the result as the new quantization table. Then, for each image block, we must select whether to apply the FM transform or the DCT.

We use a simple rule to decide whether we should apply the FM transform or not. For one bit permutations, if JPEG requires more than 64 bits for a block, we then choose to apply FM transforms instead. Similarly, for two bit permutations, if it requires more than 128 bits for a block, we then choose to apply FM transforms instead.

For one-bit permutations, we present the rate-distortion curves in Figs. 6(a) and 10(a). For two-bit permutations, we present the results in Figs. 6(b) and 10(b). For encoding the spectral coefficients we use baseline Huffman coding for all FM transforms. For computing FM transform at different bits per sample, we simply varied the *dominant_quality* parameter between 5 (producing the right endpoints), and 24 (producing the left endpoints). We show

compressed images for the sensor image in Fig. 9, and for the Mandrill image in Fig. 13. The JPEG images were computed using `cjpeg` for baseline JPEG, but also using optimized JPEG using the optimized flag for `cjpeg`.

For the sensor image, Fig. 7(b) shows the optimized JPEG image which was compressed at 1.33 bits per pixel, at a PSNR of 18.13 dB (for a quality factor of 20). For the Mandrill image, Fig. 11(b) shows the optimized JPEG image which was compressed at 1.07 bits per pixel, with a PSNR of 23.67 dB (for a quality factor of 30). As we pointed out earlier, both JPEG images suffer from severe blocking artifacts. For the sensor image, we show the one-bit FM reconstructed image in Fig. 9(a). It is compressed at 1.49 bit per pixel, with a PSNR of 18.90 dB. It corresponds to the rightmost point in the rate-distortion curve of Fig. 6(a). For the two-bit FM reconstructed image in Fig. 9(b), the image is compressed at 2.42 bits per pixel, with a PSNR of 22.50 dB. It corresponds to the leftmost point in the rate-distortion curve of Fig. 6(b).

We next explain the results for the hybrid transform. The hybrid transform was applied to the Mandrill image. The one-bit permuted image is shown in Fig. 12(a), while in Fig. 12(b), we show the two-bit permuted image. When an image block does not appear permuted, we are using JPEG for that block. When an image block is permuted, the permuted image forms the vertical stripes, and the FM transform is applied for these blocks. For one-bit permutations, we show the reconstructed image in Fig. 13(a). This image was compressed at 0.98 bits per pixel, at a PSNR of 23.89 dB. It corresponds to the leftmost point of the rate-distortion curve, for $dominant\_quality = 24.0$. Similarly, for two-bit permutations, we show the results in Fig. 13(b). This image was compressed at 1.66 bits per pixel, at a PSNR of 27.05 dB. It corresponds to the leftmost point of the rate-distortion curve, for $dominant\_quality = 24.0$.

Clearly, the FM transform provides better rate-distortion performance in Fig. 6, while the hybrid method shows better rate-distortion performance in Fig. 10. As demonstrated in Fig. 12(a) and (b), the hybrid transform worked very well, in the sense that it separated out the texture in the image for application of the FM transform, while the smooth regions were left to JPEG. The adaptive scheme seems to have worked exceptionally well for the one-bit case, while for the two bit case, our simple rule appears to be a little conservative, selecting JPEG to be applied on some blocks where the texture is not as pronounced. Overall, we believe that the hybrid method holds great promise.

VII. Conclusion

In this paper, we have demonstrated promising coding gains, especially on images containing rough, noiselike, or granular textured regions. We hope that further research in FM transform signal compression will confirm the improved performance on a large class of images. We also believe that discrete FM transforms have the potential for a broader spectrum of applications, e.g., in signal/image cryptography and general image analysis.

References

[1] A. C. Bovik, N. Gopal, T. Emmoth, and A. Restrepo, "Localized measurement of emergent image frequencies by Gabor wavelets," *IEEE Trans. Inform. Theory*, vol. 38, pp. 691–712, Mar. 1992.

[2] M. S. Pattichis and A. C. Bovik, "AM-FM expansions for images," in *Proc. Eur. Signal Processing Conf.*, Trieste, Italy, Sept. 10–13, 1996.

[3] N. D. Sidiropoulos, M. S. Pattichis, A. C. Bovik, and J. W. Havlicek, "Coperm: Transform-domain energy compaction by optimal permutation," *IEEE Trans. Image Processing*, vol. 47, pp. 1679–1688, June 1999.

[4] U. K. Laine and A. Harma, "On the design of bark-famlet filterbanks," in *Proc. Nordic Acoustical Meeting (NAM'96)*, Helsinki, Finland, June 12–14, 1996, pp. 267–276.

[5] U. K. Laine, "Famlet, to be or not to be a wavelet," in *Proc. IEEE-SP Int. Symp. Time-Frequency Time-Scale Analysis*, Victoria, BC, Canada, Oct. 4–6, 1992, pp. 335–338.

[6] U. K. Laine and T. Altosaar, "An orthogonal set of frequency and amplitude modulated (fam) functions for variable resolution signal analysis," in *Proc. IEEE Int. Conf. Acoustics, Speech, Signal Processing*, vol. 3, Albuquerque, NM, Apr. 3–6, 1990, pp. 1615–1618.

[7] R. G. Baraniuk and D. L. Jones, "Unitary equivalence: A new twist on signal processing," *IEEE Trans. Signal Processing*, vol. 43, pp. 2269–2282, Oct. 1995.

[8] I. N. Herstein, *Topics in Algebra*, 2nd ed. New York: Wiley, 1975.

[9] H. N. Shapiro, *Introduction to the Theory of Numbers*. New York: Wiley, 1983.

[10] W. B. Pennebaker and J. L. Mitchell, *JPEG Still Image Data Compression Standard*. New York: Van Nostrand Reinhold, 1993.

Marios S. Pattichis received B.S. degrees in mathematics and computer sciences in 1991, and the M.S. and Ph.D. degrees in electrical and computer engineering in 1993 and 1998, respectively, all from the University of Texas at Austin.

His research areas are focused in the general area of digital image and video processing and communication. He was a Post-Doc at the University of Texas at Austin (Summer 1998) and a Visiting Assistant Professor at Washington State University, Pullman (September 1998–August 1999). He is currently an Assistant Professor with the Department of Electrical and Computer Engineering, University of New Mexico, Albuquerque, where he is also Director of the Image and Video Processing and Communication Laboratory (IVPCL).

Alan C. Bovik (F'96) received the B.S. degree in computer engineering in 1980, and the M.S. and Ph.D. degrees in electrical and computer engineering in 1982 and 1984, respectively, all from the University of Illinois, Urbana-Champaign.

He is currently the Robert Parker Endowed Professor in the Department of Electrical and Computer Engineering, University of Texas at Austin, where he is the Associate Director of the Center for Vision and Image Sciences. During the Spring of 1992, he held a visiting position in the Division of Applied Sciences, Harvard University, Cambridge, MA. His current research interests include digital video, image processing, computer vision, wavelets, three-dimensional microscopy, and computational aspects of biological visual perception. He has published over 300 technical articles in these areas and holds two U.S. patents. He is also the editor/author of the *Handbook of Image and Video Processing* (New York: Academic, 2000).

Dr. Bovik was named Distinguished Lecturer of the IEEE Signal Processing Society in 2000, received the IEEE Signal Processing Society Meritorious Service Award in 1998, the IEEE Third Millennium Medal in 2000, the University of Texas Engineering Foundation Halliburton Award and is a two-time Honorable Mention winner of the international Pattern Recognition Society Award for Outstanding Contribution (1988 and 1993). He has been involved in numerous professional society activities, including among many others: Board of Governors, IEEE Signal Processing Society, 1996–1998; Editor-in-Chief, IEEE TRANSACTIONS ON IMAGE PROCESSING, 1996–present; and Editorial Board, PROCEEDINGS OF THE IEEE, 1998–present. He was the Founding General Chairman of the *1st IEEE International Conference on Image Processing*, which was held in Austin in November 1994. He is a registered Professional Engineer in the State of Texas and is a frequent consultant to industry and academic institutions.

John W. Havlicek received the B.S. degree in mathematics from The Ohio State University, Columbus, in 1987 and the Ph.D. degree in mathematics from Stanford University, Stanford, CA, in 1992.

He was a Visiting Research Instructor with the Mathematics Department, Michigan State University, East Lansing, from 1992 to 1995 and a Visiting Assistant Professor in the Mathematics Department, Albion College, Albion, MI, from 1995 to 1996. He is currently a Verification Engineer with Motorola, Inc.

Nicholas D. Sidiropoulos (M'92–SM'99) received the Diploma degree in electrical engineering from the Aristotelian University of Thessaloniki, Thessaloniki, Greece, and the M.S. and Ph.D. degrees in electrical engineering from the University of Maryland, College Park (UMCP), in 1988, 1990, and 1992, respectively.

From 1988 to 1992, he was a Fulbright Fellow and a Research Assistant at the Institute for Systems Research (ISR), University of Maryland, College Park. From September 1992 to June 1994 he served his military service as a Lecturer in the Hellenic Air Force Academy. From October 1993 to June 1994 he also was a Member of Technical Staff, Systems Integration Division, G-Systems Ltd., Athens, Greece. He held Postdoctoral (1994–1995) and Research Scientist (1996–1997) positions at ISR-UMCP, before joining the Department of Electrical Engineering, University of Virginia, Petersburg, in July 1997 as an Assistant Professor. He is currently an Associate Professor with the Department of Electrical and Computer Engineering, University of Minnesota, Minneapolis. His current research interests are primarily in multi-way analysis and its applications in signal processing for communications & networking.

Dr. Sidiropoulos is a member of the Signal Processing for Communications Technical Committee (SPCOM-TC) of the IEEE Signal Processing Society, and currently serves as Associate Editor for IEEE TRANSACTIONS ON SIGNAL PROCESSING and IEEE SIGNAL PROCESSING LETTERS. He received the NSF/CAREER award (Signal Processing Systems Program) in June 1998.